

**STUDY OF THERMO-DIFFUSION EFFECTS ON UNSTEADY MHD FLOW IN POROUS MEDIUM.**

---

Influence of thermal radiation, chemical reaction and heat generation effects on MHD flow with heat and mass transfer are discussed in earlier chapters. So, in this chapter, a new length is added to the mathematical analysis of MHD flow in porous medium by considering the effects of thermo-diffusion. In several transport developments in nature, flow is driven by density differences caused by temperature gradient, concentration gradient and material composition. If the mass fluxes are created by temperature gradients, it is called the Soret effect (thermal-diffusion). These effects are usually of small order of magnitude. The Soret effect shows significant role in the process of solar ponds, biological systems, and the microstructure of oceans.

This chapter contains two sections, in first section, effects of heat generation and thermo-diffusion on radiating and chemically reactive Casson fluid of MHD flow past an oscillating vertical plate in porous medium are considered. Second section of this chapter deals with Soret and parabolic motion effects on MHD flow of Second grade fluid with heat generation in porous medium with ramped boundary condition.

**6.1 SECTION I: SORET AND HEAT GENERATION EFFECTS ON MHD CASSON FLUID FLOW PAST AN OSCILLATING VERTICAL PLATE EMBEDDED THROUGH POROUS MEDIUM.**

Analytic expression for thermal diffusion and heat generation effects on MHD flow of Casson fluid past an oscillating plate embedded in porous medium with thermal radiation and chemical reaction are obtained. Ramped wall temperature with ramped surface concentration, isothermal temperature with ramped surface concentration and isothermal temperature with constant surface concentration are taken into account. The governing non-dimensional equations are solved using Laplace transform technique and the solutions are presented in closed form. In order to get a perfect understanding of the physics of the problem, numerical values of velocity, temperature and concentration profiles are obtained and presented graphically. Expression for Skin friction, Nusselt number and Sherwood number are obtained with the help of velocity, temperature and concentration profiles.

### 6.1.1 Introduction of the Problem

Such effects are important when density varies in the flow regime. For example, when species are introduced at a surface in fluid domain, with different (lower) density compared to surrounding fluid, Soret effects can be significant. Also, when heat and mass transfer take place concurrently in a moving fluid, the relations among the fluxes and the heavy potentials are of more complex nature. It has been found that an energy flux can be generated not only by temperature gradients but by composition gradients as well. Recently, Sulochana et al. [38] discussed non uniform heat source or sink effect on the flow of 3D Casson fluid in the presence of Soret and thermal radiation, whereas Nadeem et al. [120] considered thermo-diffusion effects on MHD flow of a viscoelastic fluid over a convective surface. Khan et al. [122] considered thermo-diffusion effects on MHD stagnation point flow. Many researchers like, Hayat et al. [123] and Anantha et al. [126] discussed Soret and Dufour combine effects on MHD Casson fluid flow.

Thermo-diffusion effects on MHD flow in porous medium is important phenomena in engineering and technology. Recently, Kataria and Mittal [96-97] discussed MHD flow of nano fluid past an oscillating vertical plate. Kataria and Patel [110] studied radiation and reaction effects on MHD flow of Casson fluid in porous medium. Sengupta and Ahmed [121] studied MHD flow past an oscillating plate embedded in porous media with thermal diffusion.

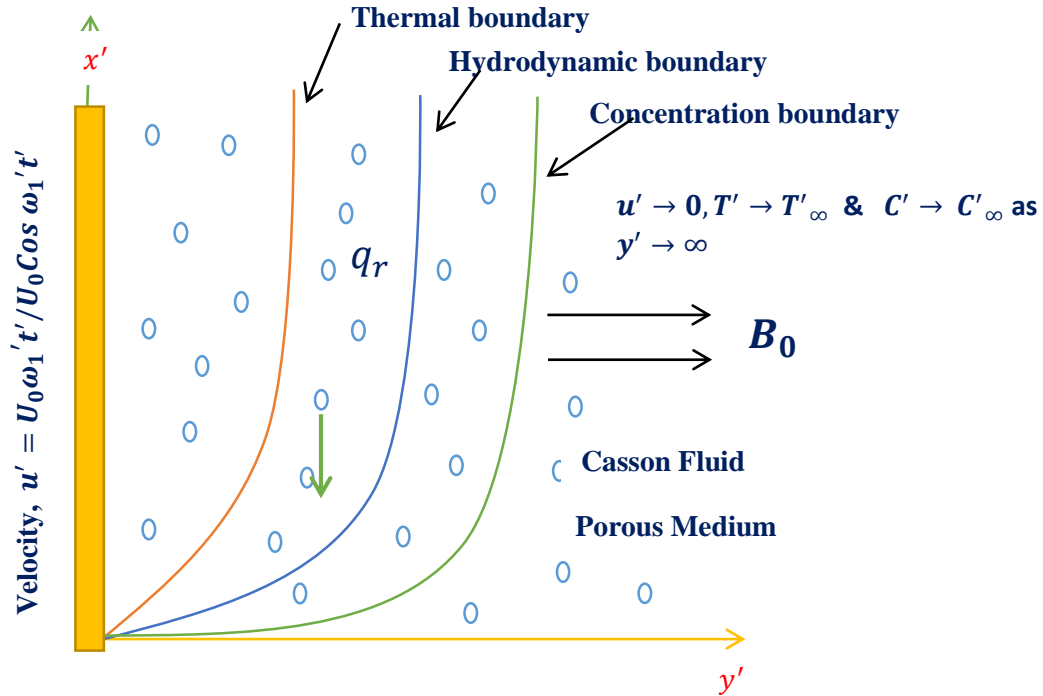
### 6.1.2 Novelty of the Problem

Novelty of this section is extension of the previous published article of Kataria and Patel [110]. So, this section is concerned with thermo-diffusion and heat generation effects on unsteady free convective MHD flow of Casson fluid in porous medium with ramped boundary conditions in energy and concentration equations. Governing equations are analytically solved using Laplace transform technique.

### 6.1.3 Mathematical Formulation of the Problem

In Figure 6.1.1, the flow being confined to  $y' > 0$ , where  $y'$  coordinate is measured in the normal direction and  $x'$  – axis is along the wall. Initially, at time  $t' = 0$ , both the fluid and the plate are at uniform temperature  $T'_{\infty}$  and the concentration near the plate is assumed to be  $C'_{\infty}$  at all the points respectively. At time  $t' > 0$ , the plate is oscillate in vertical direction against gravitational field with velocity  $U_0 \sin(\omega_1 t')$  or  $U_0 \cos(\omega_1 t')$  and constant heat flux,  $T'_{\infty} + (T'_w +$

$T'_\infty) t'/t_0$  when  $t' \leq t_0$  and  $T'_w$  when  $t' > t_0$  respectively which is there after maintained constant  $T'_w$ .



$$T' = \begin{cases} T'_\infty + (T'_w - T'_\infty) t'/t_0 & \text{if } 0 < t' < t_0 \\ T'_w & \text{if } t' \geq t_0 \end{cases}, C' = \begin{cases} C'_\infty + (C'_w - C'_\infty) t'/t_0 & \text{if } 0 < t' < t_0 \\ C'_w & \text{if } t' \geq t_0 \end{cases}; y' = 0$$

Figure 6.1.1: Physical sketch of the problem

The level of surface concentration of the plate is raised or lowered to  $C'_\infty + (C'_w + C'_\infty) t'/t_0$  when  $t' \leq t_0$  and  $C'_w$  when  $t' > t_0$  respectively which is there after maintained constant  $C'_w$ . A uniformly magnetic field of strength  $B_0$  is applied in the  $y'$  – axis direction. It is assumed that the flow of fluid is one dimensional incompressible, while induce magnetic field, electric field and viscous dissipation term in the energy equation is neglected. Under above assumptions and taking into account the Boussinesq's approximation, the governing partial differential equations are given below.

$$\rho \frac{\partial u'}{\partial t'} = \mu \beta \left( 1 + \frac{1}{\gamma} \right) \frac{\partial^2 u'}{\partial y'^2} - \sigma B_0^2 u' - \frac{\mu \phi}{k'} u' + \rho g \beta'_T (T' - T'_\infty) + \rho g \beta'_C (C' - C'_\infty) \quad (6.1.1)$$

$$\frac{\partial T'}{\partial t'} = \frac{k_4}{\rho c_p} \frac{\partial^2 T'}{\partial y'^2} - \frac{1}{\rho c_p} \frac{\partial q_r}{\partial y'} + \frac{Q_0}{\rho c_p} (T' - T'_\infty) \quad (6.1.2)$$

$$\frac{\partial C'}{\partial t'} = D_M \frac{\partial^2 C'}{\partial y'^2} + D_T \frac{\partial^2 T'}{\partial y'^2} - k'_2 (C' - C'_\infty) \quad (6.1.3)$$

with following initial and boundary conditions:

$$u' = 0, T' = T'_\infty, C' = C'_\infty; \text{ as } y' \geq 0 \text{ and } t' \leq 0, \quad (6.1.4)$$

$$u' = U_0 \sin(\omega_1 t') \text{ or } U_0 \cos(\omega_1 t'), T' = \begin{cases} T'_\infty + (T'_w - T'_\infty) t'/t_0 & \text{if } 0 < t' < t_0, \\ T'_w & \text{if } t' \geq t_0 \end{cases},$$

$$C' = \begin{cases} C'_\infty + (C'_w - C'_\infty) t'/t_0 & \text{if } 0 < t' < t_0, \\ C'_w & \text{if } t' \geq t_0 \end{cases}; \text{ as } t' > 0 \text{ and } y' = 0, \quad (6.1.5)$$

$$u' \rightarrow 0, T' \rightarrow T'_\infty, C' \rightarrow C'_\infty; \text{ as } y' \rightarrow \infty \text{ and } t' \geq 0 \quad (6.1.6)$$

where

$$y = \frac{y'}{U_0 t_0}, u = \frac{u'}{U_0}, t = \frac{t'}{t_0}, \theta = \frac{(T' - T'_\infty)}{(T'_w - T'_\infty)}, C = \frac{(C' - C'_\infty)}{(C'_w - C'_\infty)}, Gr = \frac{\nu g \beta'_T (T'_w - T'_\infty)}{U_0^3}$$

$$Gm = \frac{\nu g \beta'_C (C'_w - C'_\infty)}{U_0^3}, M = \frac{\sigma B_0^2 \nu}{\rho U_0^2}, Pr = \frac{\rho \nu C_p}{k_4}, Nr = -\frac{16 a \sigma \nu^2 T'^3_\infty}{k_4 U_0^2}, H = \frac{Q_0 \nu^2}{k_4 U_0^2}, Sc = \frac{\nu}{D_M}$$

$$Kr = \frac{\nu k'_2}{U_0^2}, Sr = \frac{D_T (T'_w - T'_\infty)}{\nu (C'_w - C'_\infty)}, \gamma = \frac{\mu_B \sqrt{2\pi c}}{P_y}, \tau = \frac{\tau}{\rho u^2}, \frac{\partial q_r}{\partial y'} = -4a^* \sigma^* (T'^4_\infty - T'^4), T'^4 \cong$$

$$4T'^3_\infty T' - 3T'^4_\infty$$

In the equations (6.1.1) to (6.1.3) dropping out the " ' " notation (for simplicity),

$$\frac{\partial u}{\partial t} = \left(1 + \frac{1}{\gamma}\right) \frac{\partial^2 u}{\partial y^2} - \left(M^2 + \frac{1}{k}\right) u + G_r \theta + G_m C \quad (6.1.7)$$

$$\frac{\partial \theta}{\partial t} = \frac{1}{Pr} \frac{\partial^2 \theta}{\partial y^2} + \frac{(H - Nr)}{Pr} \theta \quad (6.1.8)$$

$$\frac{\partial C}{\partial t} = \frac{1}{Sc} \frac{\partial^2 C}{\partial y^2} + Sr \frac{\partial^2 \theta}{\partial y^2} - krC \quad (6.1.9)$$

with initial and boundary condition

$$u = \theta = C = 0, y \geq 0, t \leq 0, u = \cos \omega_1 t / \sin \omega_1 t \text{ at } y = 0, t > 0$$

$$, \theta = \begin{cases} t, & 0 < t \leq 1 \\ 1 & t > 1 \end{cases}, C = \begin{cases} t, & 0 < t \leq 1 \\ 1 & t > 1 \end{cases} \text{ at } y = 0, t > 0,$$

$$u \rightarrow 0, \theta \rightarrow 0, C \rightarrow 0 \text{ at } y \rightarrow \infty, t > 0 \quad (6.1.10)$$

### 6.1.4 Solution of the Problem

Exact expression for fluid velocity, temperature and concentration profiles are obtained from equations (6.1.7) to (6.1.9) with initial boundary condition (6.1.10) using the Laplace transform technique.

#### 6.1.4.1 Solution of the problem for ramped temperature and ramped surface concentration

$$\theta(y, t) = f_9(y, t) - f_9(y, t - 1)H(t - 1) \quad (6.1.11)$$

$$C(y, t) = h_2(y, t) - h_2(y, t - 1)H(t - 1) \quad (6.1.12)$$

$$u(y, t) = g_1(y, t) + h_1(y, t) - h_1(y, t - 1)H(t - 1) \quad (6.1.13)$$

#### 6.1.4.2 Solution of the problem for isothermal temperature and ramped surface concentration

In this case, the initial and boundary conditions are the same excluding equations (6.1.10) that becomes  $\theta = 1$  at  $y = 0, t \geq 0$ . For this case, expression for velocity, temperature and concentration profiles are derived which is given below.

$$\theta(y, t) = f_8(y, t) \quad (6.1.14)$$

$$C(y, t) = f_{13}(y, t) - f_{13}(y, t - 1)H(t - 1) + g_{12}(y, t) - g_{13}(y, t) \quad (6.1.15)$$

$$u(y, t) = g_1(y, t) + g_5(y, t) + g_6(y, t) - g_6(y, t - 1)H(t - 1) + g_7(y, t) - g_8(y, t) + g_8(y, t - 1)H(t - 1) - g_9(y, t) \quad (6.1.16)$$

#### 6.1.4.3 Solution of the problem for isothermal temperature and constant concentration

In this case, the initial and boundary conditions are the same excluding equations (6.1.10) that becomes  $C = 1, \theta = 1$  at  $y = 0, t \geq 0$ . Expression for velocity, temperature and concentration profiles are obtained for these case which can be written as,

$$\theta(y, t) = f_8(y, t) \quad (6.1.17)$$

$$C(y, t) = f_{12}(y, t) + g_{12}(y, t) - g_{13}(y, t) \quad (6.1.18)$$

$$u(y, t) = h_3(y, t) \quad (6.1.19)$$

#### 6.1.4.4 Nusselt number, Sherwood number and Skin friction

Expressions for Nusselt number  $Nu$ , Sherwood number  $Sh$  and Skin friction  $\tau$  for all thermal plates are calculated from equation (6.1.11) to equation (6.1.19) respectively using the relation

$$Nu = -\frac{v}{U_0(T'-T'_\infty)} \left( \frac{\partial T'}{\partial y'} \right)_{y'=0}, Sh = -\frac{v}{U_0(C'-C'_\infty)} \left( \frac{\partial C'}{\partial y'} \right)_{y'=0} \text{ and } \tau^*(y, t) = -\mu_B \left( 1 + \frac{1}{\gamma} \right) \tau,$$

$$\text{where } \tau = \left. \frac{\partial u}{\partial y} \right|_{y=0} \quad (6.1.20)$$

For ramped wall temperature and ramped surface concentration:

$$Nu = -[J_9(t) - J_9(t-1)H(t-1)] \quad (6.1.21)$$

$$Sh = -[J_{32}(t) - J_{32}(t-1)H(t-1)] \quad (6.1.22)$$

$$\tau = J_{16}(t) + J_{31}(t) - J_{31}(t-1)H(t-1) \quad (6.1.23)$$

For isothermal temperature and constant surface concentration:

$$Nu = -[J_8(t)] \quad (6.1.24)$$

$$Sh = -[J_{13}(t) - J_{13}(t-1)H(t-1) + J_{27}(t) - J_{28}(t)] \quad (6.1.25)$$

$$\tau = J_{16}(t) + J_{20}(t) + J_{21}(t) - J_{21}(t-1)H(t-1) + J_{22}(t) - J_{23}(t) + J_{23}(t-1)H(t-1) - J_{24}(t) \quad (6.1.26)$$

For isothermal temperature and constant surface concentration:

$$Nu = -[J_8(t)] \quad (6.1.27)$$

$$Sh = -[J_{12}(t) + J_{27}(t) - J_{28}(t)] \quad (6.1.28)$$

$$\tau = J_{33}(t) \quad (6.1.29)$$

### 6.1.5 Result and Discussion

To understand of influence for different physical parameters, numerical values of velocity, temperature and concentration profiles are obtained from analytic results and presented graphically through Figure 6.1.2 to Figure 6.1.12.

Effect of Casson fluid parameter  $\gamma$  on velocity profiles is shown in Figure 6.1.2. It is found that velocity decrease with increasing values of  $\gamma$ . Figure 6.1.3 shows that velocity decreases with increase in  $M$ . This is due to the fact that the application of a magnetic field to an electrically conducting fluid gives increase to a resistive force called Lorentz force which has a tendency to slow down the motion of fluid. Figure 6.1.4 displays velocity profile for different values of porous

medium  $k$ . When the porous medium parameter  $k$  increased, holes become larger and therefore motion of the fluid rises.

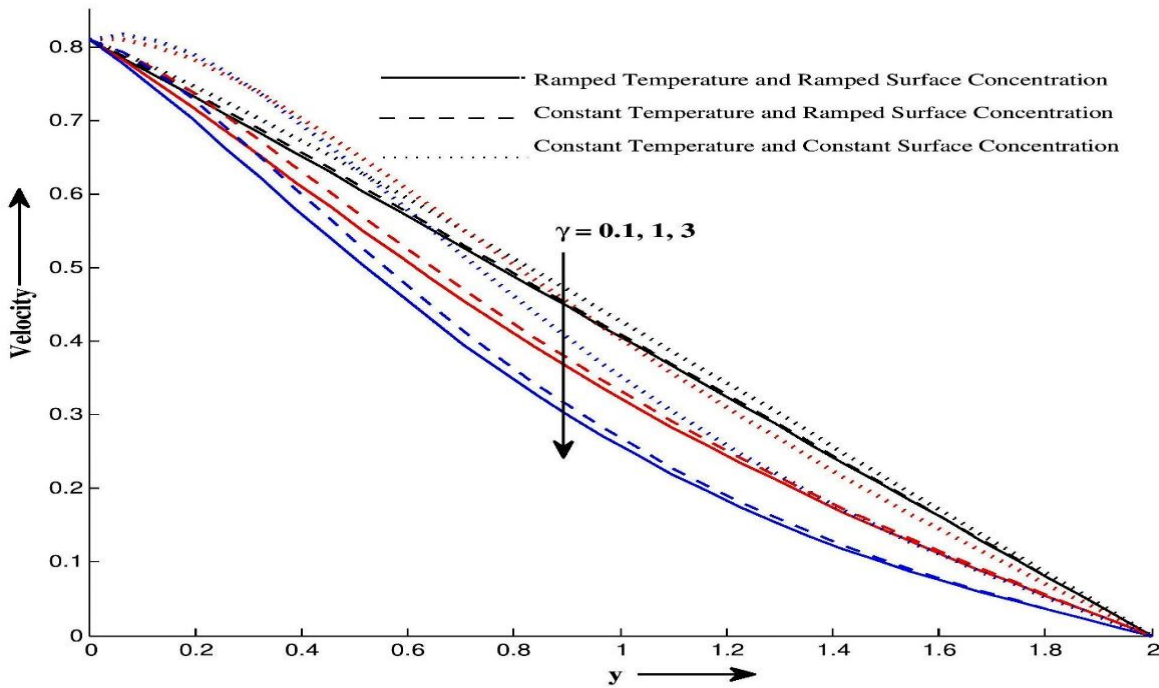


**Figure 6.1.2:** Velocity profile  $u$  for different values of  $y$  and  $\gamma$  at  $Pr = 25, M = 0.5, k = 1, Sc = 0.66, Gm = 2, Gr = 4, Nr = 5, Kr = 4, H = 5, Sr = 7$  and  $t = 0.4$ .

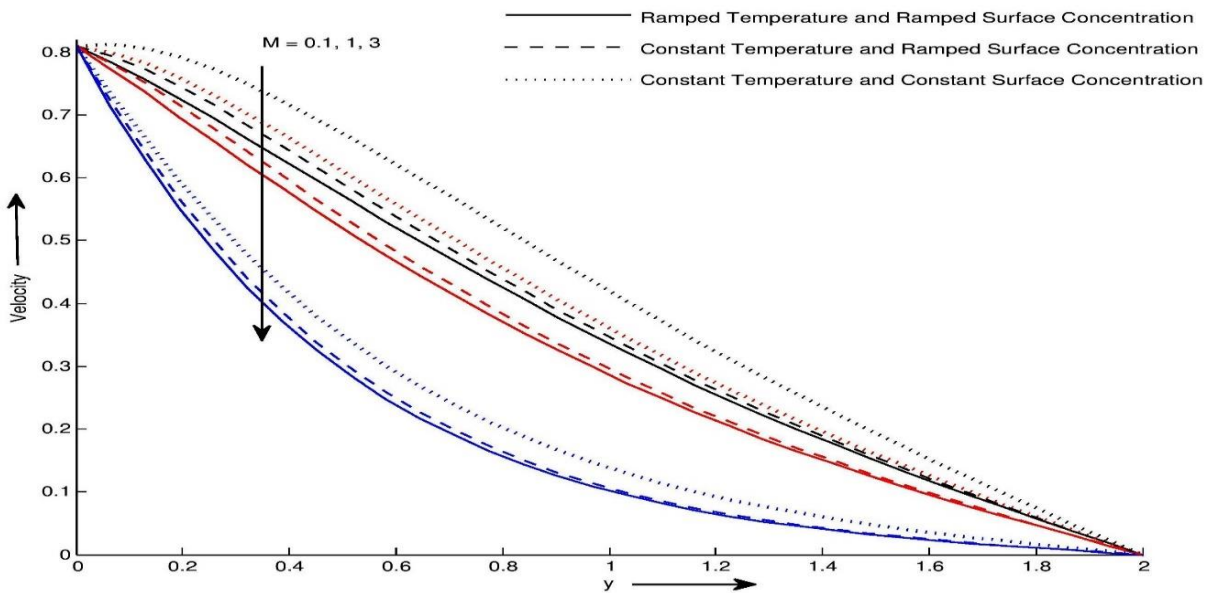


**Figure 6.1.3:** Velocity profile  $u$  for different values of  $y$  and  $M$  at  $\gamma = 1, Pr = 25, k = 1, Sc = 0.66, Gm = 2, Gr = 4, Nr = 5, Kr = 4, H = 5, Sr = 7$  and  $t = 0.4$

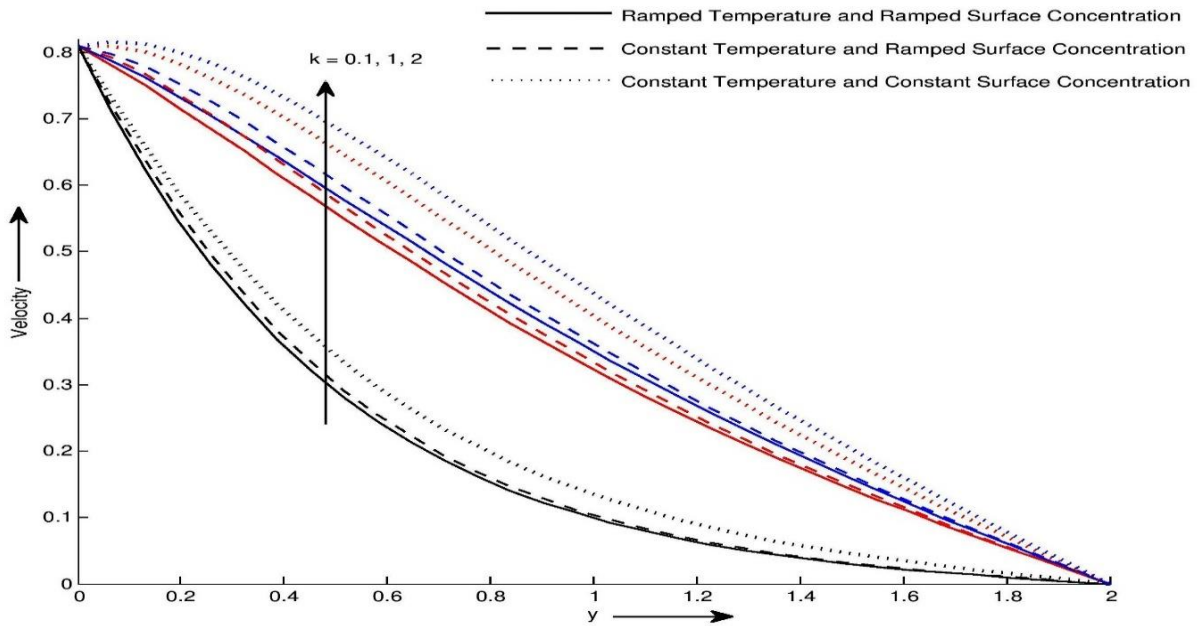


**Figure 6.1.4:** Velocity profile  $u$  for different values of  $y$  and  $k$  at  $\gamma = 1, M = 0.5, Pr = 25,$   
 $Sc = 0.66, Gm = 2, Gr = 4, Nr = 5, Kr = 4, H = 5, Sr = 7$  and  $t = 0.4$

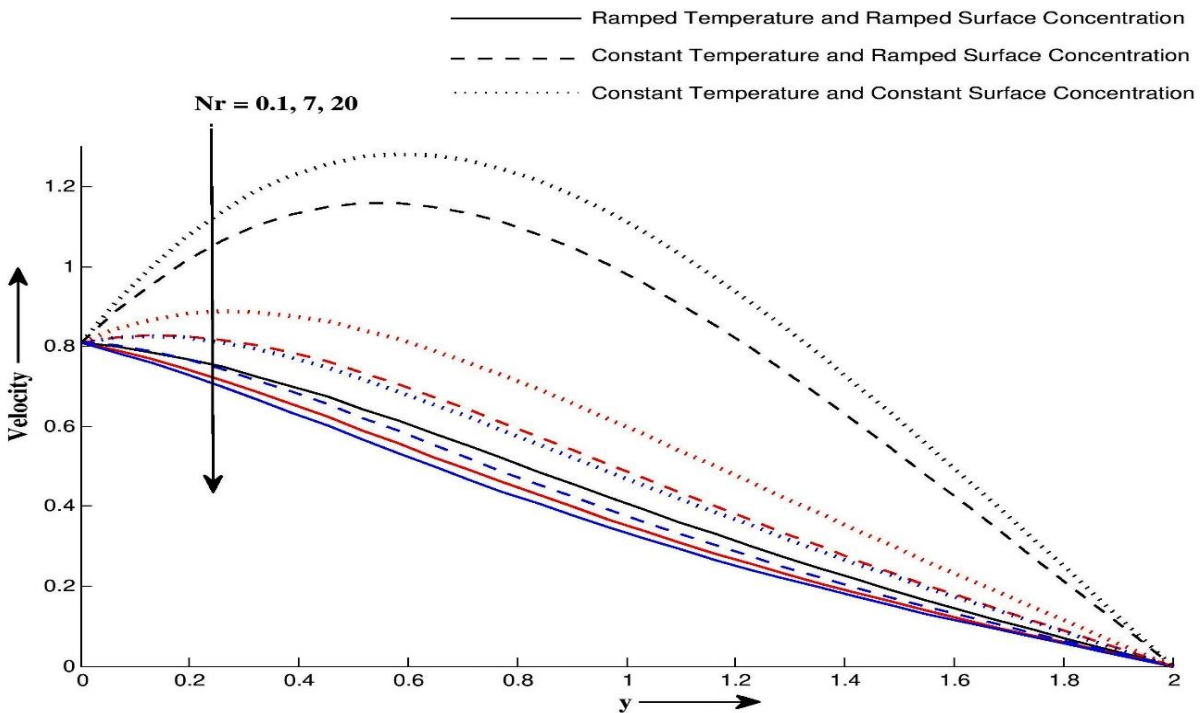


**Figure 6.1.5:** Velocity profile  $u$  for different values of  $y$  and  $Nr$  at  $\gamma = 1, M = 0.5, k = 1,$   
 $Sc = 0.66, Gm = 2, Pr = 0.71, Kr = 4, H = 5, Sr = 7$  and  $t = 0.4$ .

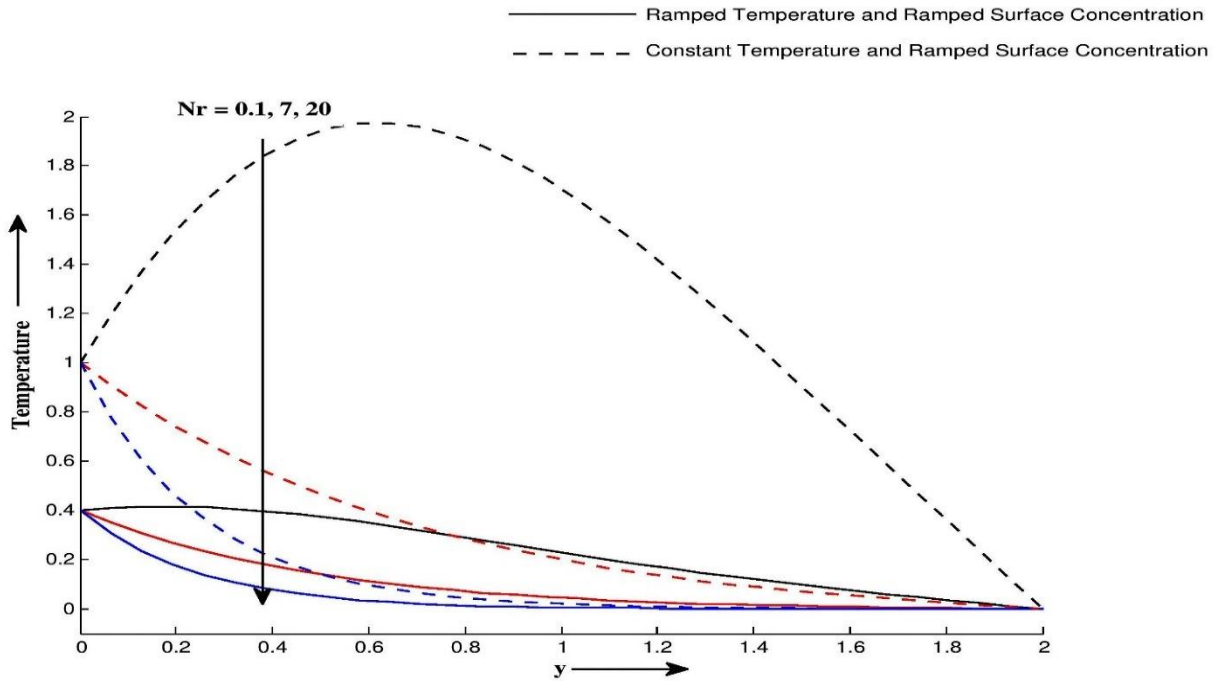


Figure 6.1.6: Temperature profile  $\theta$  for different values of  $y$  and  $Nr$  at  $Pr = 0.71, H = 5$  and  $t = 0.4$

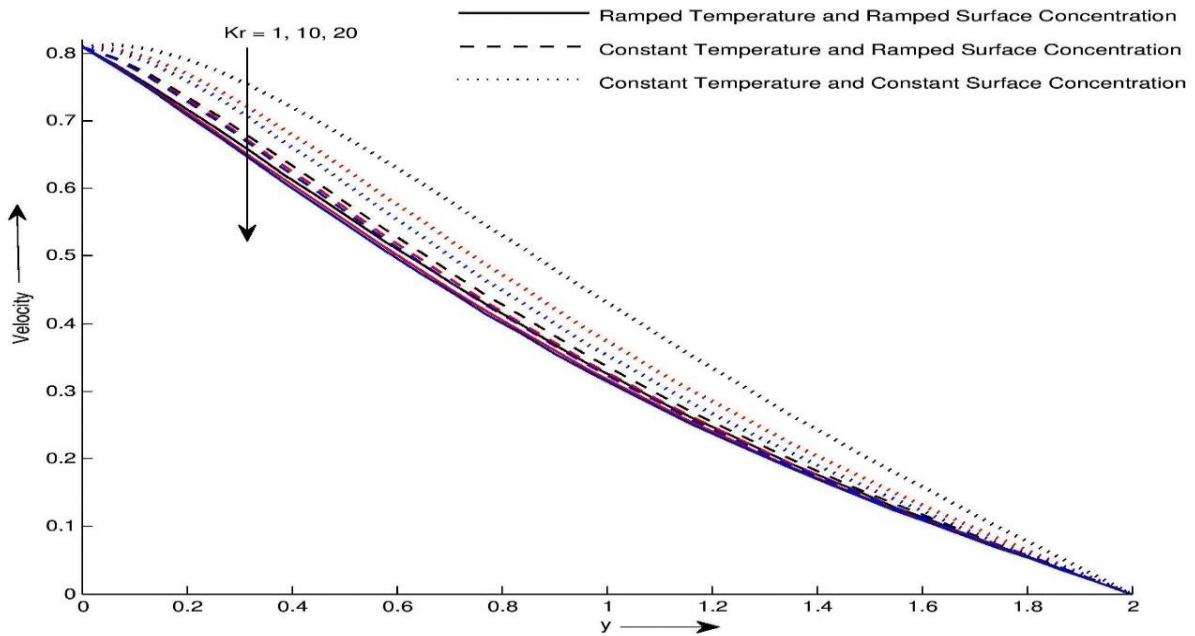
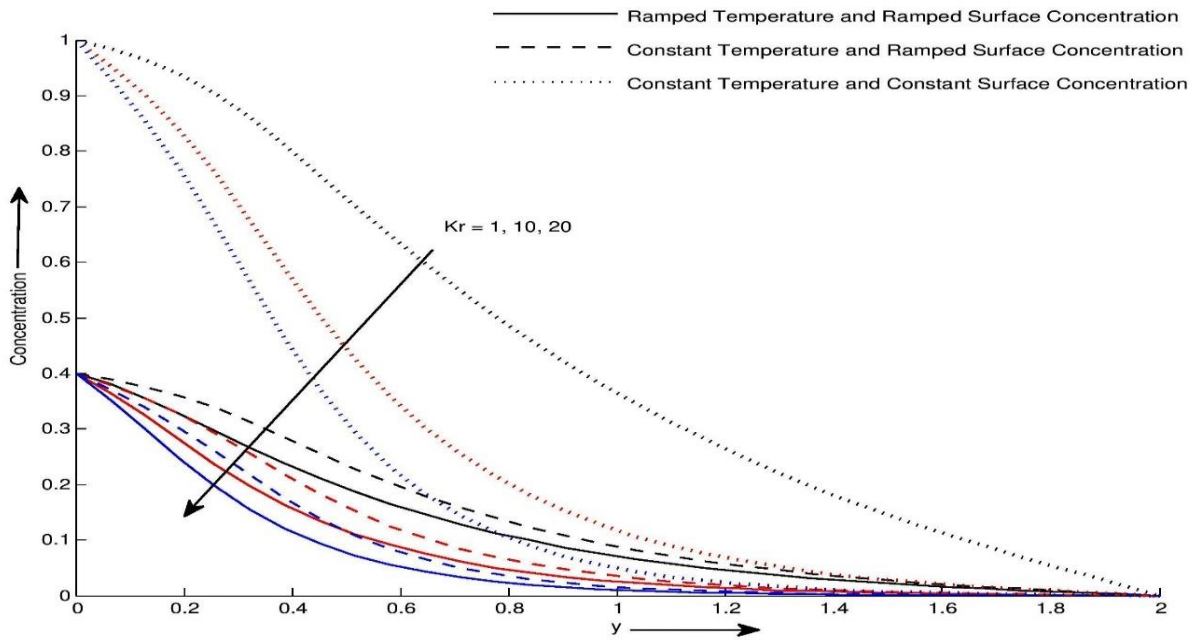
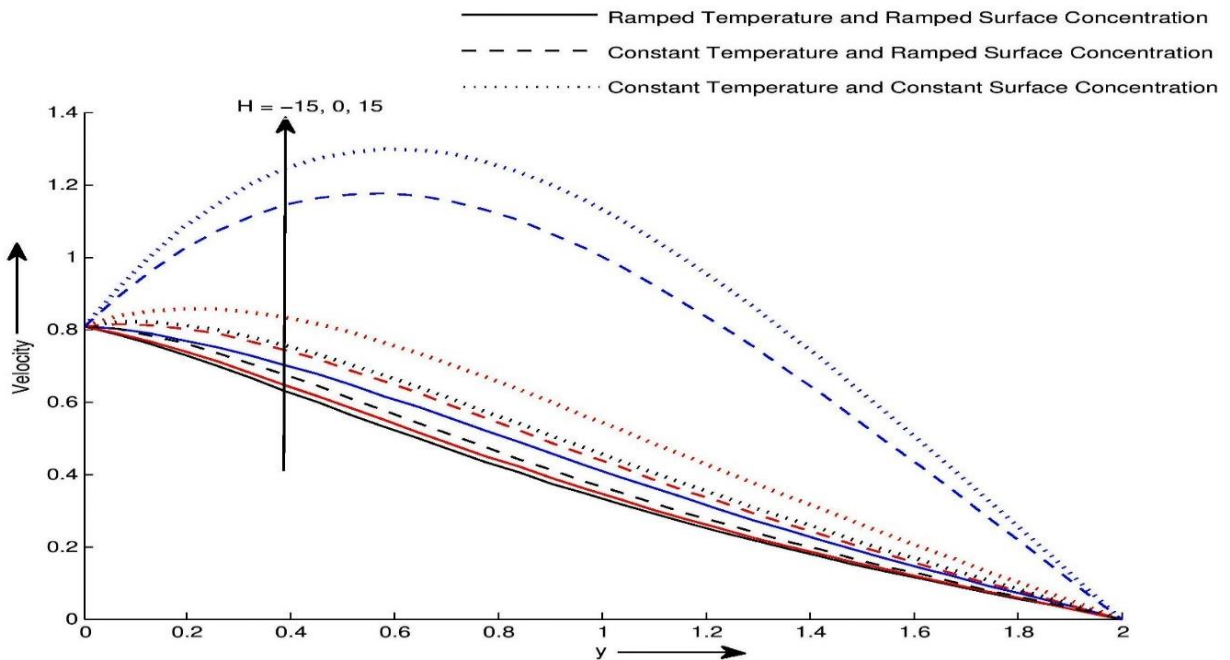


Figure 6.1.7: Velocity profile  $u$  for different values of  $y$  and  $Kr$  at  $\gamma = 1, M = 0.5, k = 1, Sc = 0.66, Gm = 2, Gr = 4, R = 5, Pr = 25, H = 5, Sr = 7$  and  $t = 0.4$



**Figure 6.1.8:** Concentration profile  $C$  for different values of  $y$  and  $Kr$  at  $Gm = 2, Gr = 4, Nr = 5, Sc = 0.66, H = 5, Sr = 7, Pr = 25$  and  $t = 0.4$ .



**Figure 6.1.9:** Velocity profile  $u$  for different values of  $y$  and  $H$  at  $\gamma = 1, M = 0.5, k = 1, Sc = 0.66, Gm = 2, Gr = 4, Nr = 5, Pr = 0.71, H = 5, Sr = 7$  and  $t = 0.4$

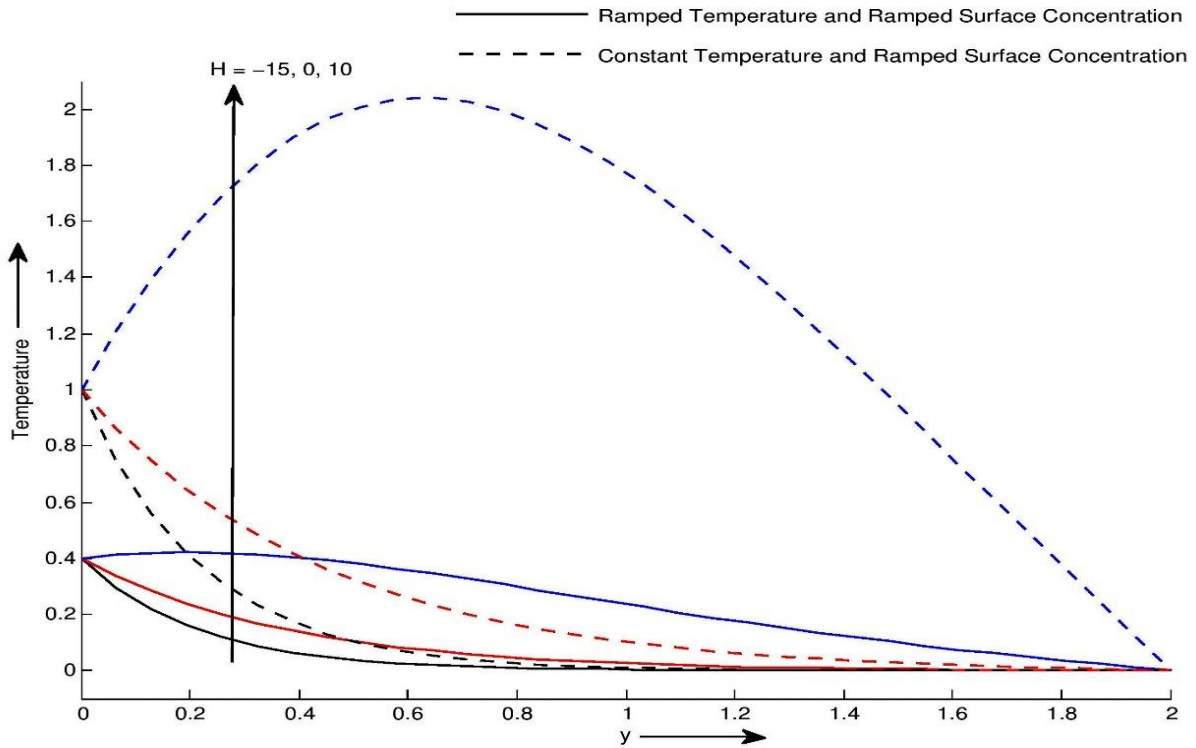


**Figure 6.1.10:** Temperature profile  $\theta$  for different values of  $y$  and  $H$  at  $Nr = 5, Pr = 0.71$  and  $t = 0.4$ .

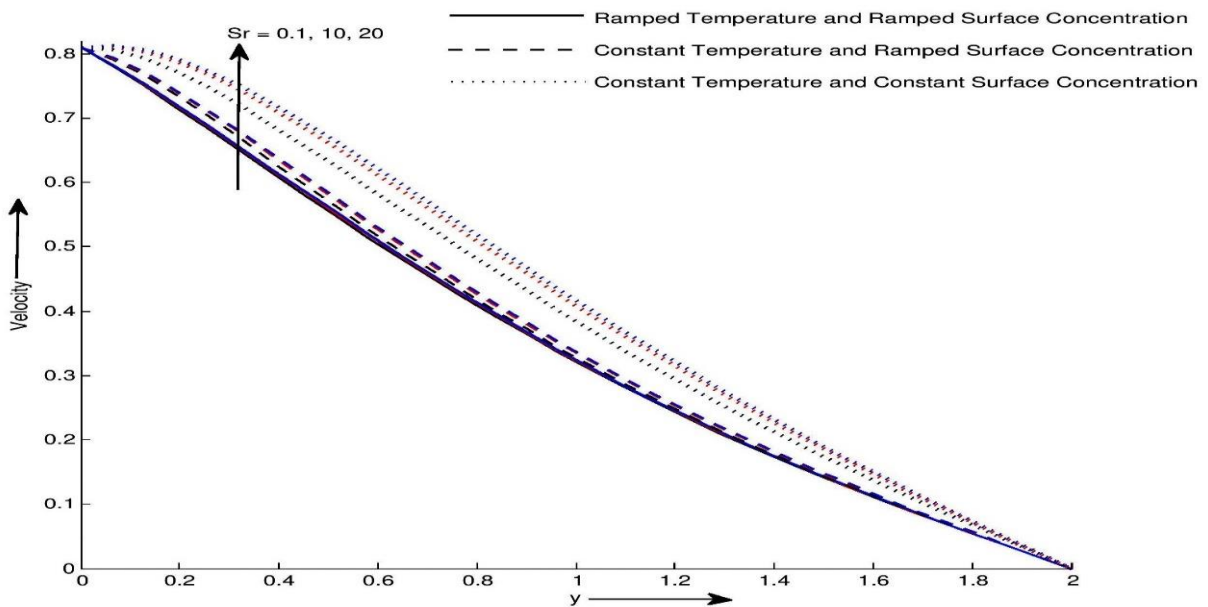


**Figure 6.1.11:** Velocity profile  $u$  for different values of  $y$  and  $Sr$  at  $\gamma = 1, M = 0.5, k = 1, Sc = 0.66, Gm = 2, Gr = 4, Nr = 5, Kr = 4, H = 16, Pr = 25$  and  $t = 0.4$

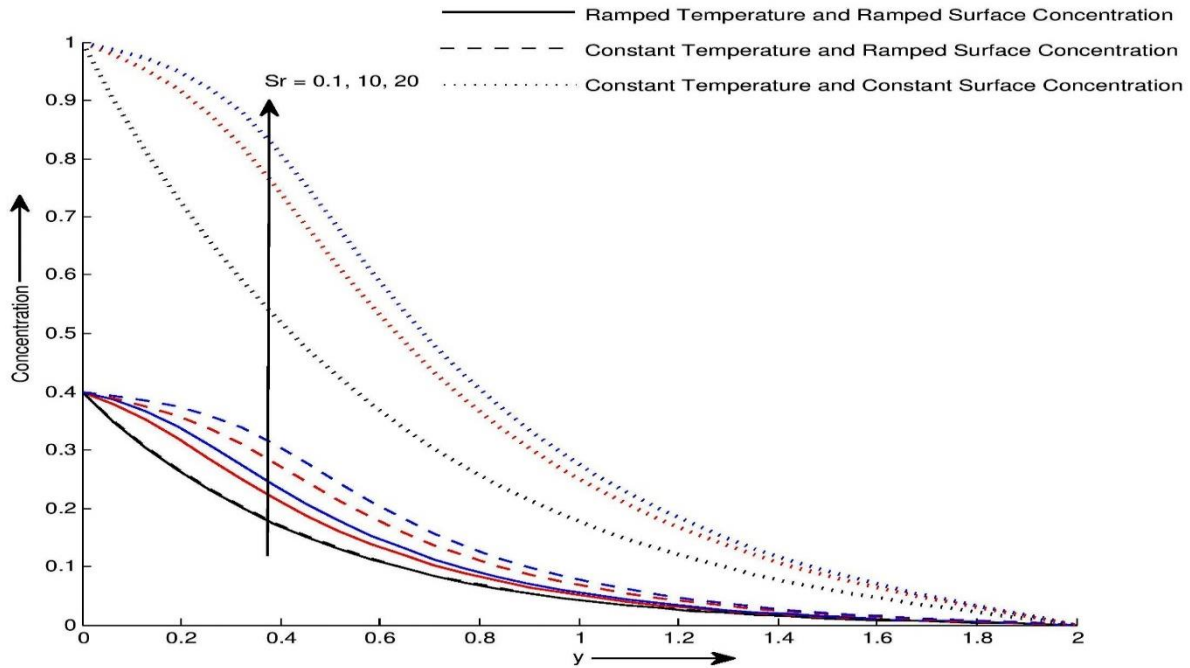


**Figure 6.1.12:** Concentration profile  $C$  for different values of  $y$  and  $Sr$  at  $Gm = 2, Gr = 4,$   
 $Nr = 5, Kr = 4, H = 5, Pr = 25$  and  $t = 0.4$

Figure 6.1.5 and Figure 6.1.6 shows effect of radiation parameter  $Nr$  on velocity and temperature profiles. It is observed that velocity and temperature profiles has decreasing tendency with  $Nr$ . If dimensionless quantity  $Nr = \frac{16 a^* \sigma^* v^2 T'_{\infty}{}^3}{k_4 U_0^2}$  instead of  $Nr = -\frac{16 a^* \sigma^* v^2 T'_{\infty}{}^3}{k_4 U_0^2}$  is considered in energy equation 4.1.9 then velocity and temperature increases with increase in  $Nr$ . It is noticed that thermal radiation parameter reduces thermal buoyancy force, minimizing the thickness of the thermal boundary layer. Figure 6.1.7 and Figure 6.1.8 shows effect of chemical reaction on velocity and concentration profiles for all boundary conditions. It is seen that, velocity and concentration decreases with increase in chemical reaction parameter  $Kr$ . This shows that the destructive reaction leads to decrease in the concentration field which in turn fails the buoyancy effects due to concentration gradients. This result is strongly agreed with kataria and Patel [110]. Effect of Heat generation parameter  $H$  on velocity and temperature profiles are described in Figure 6.1.9 and Figure 6.1.10. It is noticed that velocity and temperature profiles has increasing tendency with  $H$ . Heat source implies generation of heat from the surface of the region, which rises the temperature in the flow field. Therefore, as heat generation parameter increased, the temperature will be increases, then motion of the fluid is obviously increased. For all boundary conditions, heat transfer process is

faster with increase in heat generation parameter  $H$ . Figure 6.1.11 and Figure 6.1.12 exhibits effects of thermal-diffusion on velocity and concentration profiles for all boundary conditions. It is observed from these figures that the velocity and concentration profiles of the fluid gets faster by the rise in values of Soret number. Increase in values of Soret number, raises the mass buoyancy force which results an increase in the value of velocity.

**Table 6.1.1:** Skin friction variation

$\gamma$	$Sr$	$M$	$k$	$t$	$\tau$ for Ramped temperature with Ramped Concentration	$\tau$ for isothermal temperature with Ramped Concentration	$\tau$ for constant temperature with constant concentration
0.1	0.2	0.1	1	0.4	-0.4813	-0.4779	-0.5548
0.15	0.2	0.1	1	0.4	-0.3481	-0.4018	-0.6887
0.2	0.2	0.1	1	0.4	-0.2580	-0.3587	-0.7975
0.1	0.3	0.1	1	0.4	-0.5503	-0.4807	-0.5576
0.1	0.4	0.1	1	0.4	-0.6194	-0.4834	-0.5604
0.1	0.2	0.2	1	0.4	-0.4679	-0.4669	-0.5574
0.1	0.2	0.3	1	0.4	-0.4475	-0.4502	-0.5617
0.1	0.2	0.1	1.1	0.4	-0.5284	-0.5165	-0.5469
0.1	0.2	0.1	1.2	0.4	-0.5774	-0.5567	-0.5403
0.1	0.2	0.1	1	0.5	-0.5891	-0.5765	-0.5557
0.1	0.2	0.1	1	0.6	-0.6960	-0.6735	-0.5601

**Table 6.1.2:** Nusselt number variation

$Pr$	$Nr$	$H$	$t$	$Nu$ for Ramped Temperature	$Nu$ for isothermal Temperature
15	7	5	0.4	0.1924	-2.9134
16	7	5	0.4	0.1866	-3.0433
17	7	5	0.4	0.1812	-3.1682
15	7.1	5	0.4	0.2018	-2.8869

15	7.2	5	0.4	0.2112	-2.8605
15	7	5.5	0.4	0.1451	-3.0467
15	7	6.0	0.4	0.0972	-3.1814
15	7	5	0.5	0.2675	-2.4878
15	7	5	0.6	0.3498	-2.1645

**Table 6.1.3:** Sherwood number variation

$Nr$	$Sr$	$H$	$t$	$Sh$ for Ramped temperature with Ramped Concentration	$Sh$ for isothermal temperature with Ramped Concentration	$Sh$ for constant temperature with constant concentration
7	0.2	5	0.4	4.9522	0.1098	-0.2587
7.1	0.2	5	0.4	3.7547	0.1082	-0.2604
7.2	0.2	5	0.4	2.6888	0.1066	-0.2620
7	0.3	5	0.4	15.7829	0.1563	-0.2122
7	0.4	5	0.4	26.6137	0.2029	-0.1657
7	0.2	5.5	0.4	13.9757	0.1179	-0.2507
7	0.2	6.0	0.4	34.9673	0.1260	-0.2425
7	0.2	5	0.5	4.1610	0.0997	-0.2279
7	0.2	5	0.6	3.5609	0.0941	-0.2049

The variations of the Skin friction, Nusselt number and Sherwood number are shown in Table 6.1.1 to Table 6.1.3 for several values of the governing parameters. Table 6.1.2 shows effect of  $Pr$ ,  $H$  and time  $t$  on temperature gradient at the surface. For all thermal cases, prandtl number and heat source parameter tend to reduce the magnitude of Nusselt number while time variable  $t$  has reverse effects on it. Table 6.1.3 indicates magnitude of concentration gradient at the surface. For all thermal cases, radiation and time variable tends to reduce the values of Sherwood number while Soret number and heat source parameter has reverse effect on it. Table 6.1.1 illustrate that the magnitude of Skin friction decreases with increase in  $Sr$  and  $t$ . It is also seen that, Skin friction increases with increase in Casson parameter  $\gamma$  and magnetic field  $M$  while decreases with increase in porous medium  $k$ . For

constant temperature and surface concentration, Casson fluid  $\gamma$  and magnetic field  $M$  tends to reduce Skin friction while permeability of porous medium  $k$  has reverse effect on it.

### 6.1.6 Concluding Remark

The most important concluding remarks can be summarized as follows:

- It is observed that magnitude of momentum, heat and mass transfer in case of ramped temperature with ramped surface concentration is less than that of isothermal temperature with ramped surface concentration.
- It is observed that magnitude of momentum, heat and mass transfer in case of constant temperature with ramped surface concentration is less than that of constant temperature with constant surface concentration.
- Motion of fluid decrease tendency with Casson parameter  $\gamma$ , chemical reaction  $Kr$ , thermal radiation  $Nr$  and increase tendency with heat generation  $H$  and thermal diffusion  $Sr$ .
- Temperature decreases with thermal radiation parameter  $Nr$  and increases with Heat generation  $H$
- Concentration decreases tendency with chemical reaction parameter  $Kr$  and increase with Soret number  $Sr$ .

## 6.2 SECTION II: EFFECT OF THERMO-DIFFUSION AND PARABOLIC MOTION ON MHD SECOND GRADE FLUID FLOW WITH RAMPED WALL TEMPERATURE AND RAMPED SURFACE CONCENTRATION

In this section, parabolic motion, heat generation/absorption and thermo-diffusion effects on unsteady free convective MHD flow of Second grade fluid near an infinite vertical plate in porous medium has been considered. It is presumed that the plate has a ramped temperature as well as isothermal temperature. For finding the exact solution, Laplace transform technique is applied on the governing dimensionless equations. Analytic expression of Skin friction, Nusselt number and Sherwood number are derived and represented in tabular form. The effects of Magnetic parameter  $M$ , Second grade fluid  $\alpha$ , Heat generation/absorption  $H$ , thermal radiation parameter  $Nr$ , chemical reaction  $Kr$  and thermo-diffusion  $Sr$  on velocity, temperature and concentration profiles are discussed through several figures.

### 6.2.1 Introduction of the Problem

There are many applications for the parabolic motion such as in solar cookers, solar concentrators and parabolic through solar collector. A parabolic concentrator type solar cooker has a wide range of applications like baking, roasting and distillation. Solar concentrators have their applications in increasing the rate of evaporation of waste water, in food processing, for making drinking water from brackish and sea water. Murty et al. [41] studied evaluation of thermal performance of heat exchanger unit for parabolic solar cooker, while Raja et al. [42] deals with design and manufacturing of parabolic through solar collector system. Muthucumaraswamy and Geetha [43] considered effects of parabolic motion on vertical plate with constant mass flux.

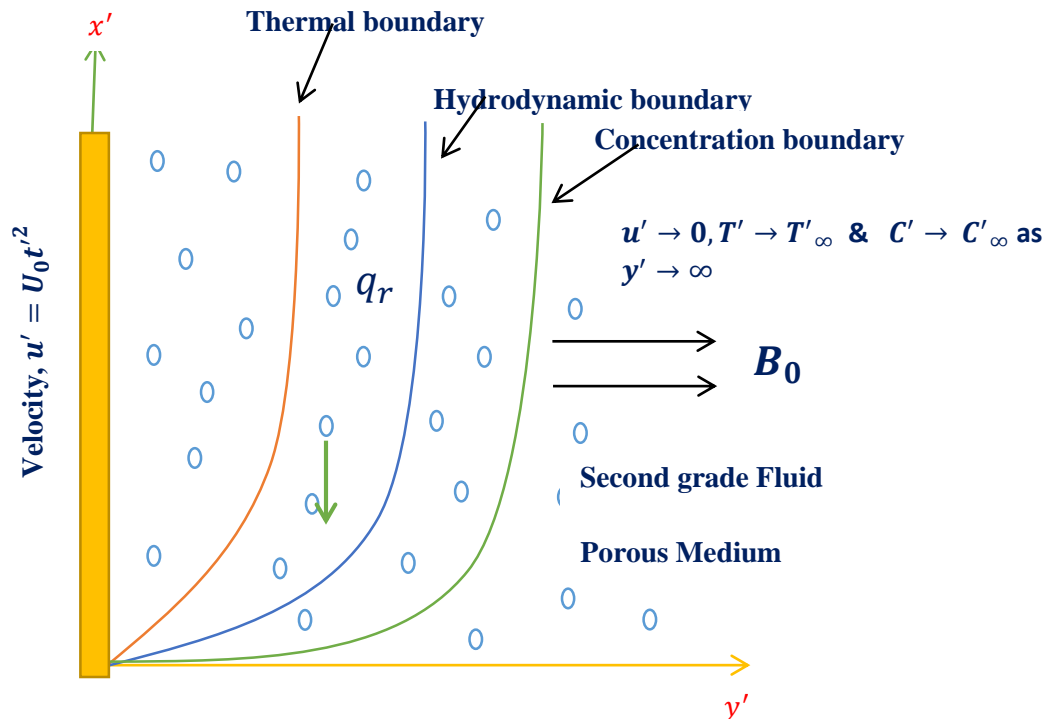
Recently, Das et al. [80] discussed Second grade fluid of MHD flow over a convectively heated stretching sheet. Hayat et al. [82] obtained the solution of Second grade fluid flow with magnetic field in a porous channel. Samiulhaq et al. [155], Kataria and Patel [156] discussed MHD flow of Second grade fluid through porous medium with ramped wall temperature. Olanrewaju and Abbas [128] studied effect of thermal radiation and thermal diffusion on MHD Second grade fluid flow. Sengupta and Ahmed [121] deals MHD flow with thermal diffusion through embedded in porous media, whereas Kataria and Patel [127] studied thermo-diffusion and heat generation effects on MHD Casson fluid flow with radiation and reaction in porous medium.

### 6.2.2 Novelty of the problem

Our work can be considered as extension of investigation carried out by Samiulhaq et al. [155] and Kataria and Patel [156]. So, Novelty of this section is mathematical analysis of parabolic motion, thermo-diffusion and Heat generation/absorption effects on MHD Second grade fluid flow near an infinite vertical plate in porous medium. It is considered the plate has a ramped temperature with ramped surface concentration and isothermal temperature with ramped surface concentration. As analytical solution is discussed, unlike numerical work of different authors, convergence of solution is not an issue.

### 6.2.3 Mathematical Formulation of the Problem

As shown in Figure 6.2.1, coordinate system is chosen such that  $x'$  – axis is along the wall in upward direction and  $y'$  – axis is normal to it.



$$T' = \begin{cases} T'_\infty + (T'_w - T'_\infty) t'/t_0 & \text{if } 0 < t' < t_0 \\ T'_w & \text{if } t' \geq t_0 \end{cases}, C' = \begin{cases} C'_\infty + (C'_w - C'_\infty) t'/t_0 & \text{if } 0 < t' < t_0 \\ C'_w & \text{if } t' \geq t_0 \end{cases}; y' = 0$$

Figure 6.2.1: Physical sketch of the problem

A uniform magnetic field of strength  $B_0$  is acting in transverse direction to the flow as shown in Figure 6.2.1. Initially, at time  $t' \leq 0$ , both the fluid and the plate are at rest to a constant temperature  $T'_\infty$  and the concentration at the surface is assumed to be  $C'_\infty$  respectively. At the time  $t' > 0$ , the temperature of the plate is either raised or lowered to  $T'_\infty + (T'_w - T'_\infty) t'/t_0$  when  $t' \leq t_0$ , and thereafter, for  $t' > t_0$ , is maintained at the constant temperature  $T'_w$ . The level of concentration at the surface of the wall is either raised or lowered to  $C'_\infty + (C'_w - C'_\infty) t'/t_0$  when  $t' \leq t_0$  and thereafter, for  $t' > t_0$  is maintained constant surface concentration  $C'_w$  respectively. It is supposed that the viscous dissipation, induce magnetic and electrical field effects are negligible.

One of the body force terms corresponding to MHD flow is the Lorentz force  $J \times B = \sigma B_0^2 u$ , Under above assumptions and taking into account the Boussinesq's approximation, governing equations are given below:

$$\frac{\partial u'}{\partial t'} = \left( \nu + \frac{\alpha_1}{\rho} \frac{\partial}{\partial t'} \right) \frac{\partial^2 u'}{\partial y'^2} + g\beta'_T (T' - T'_\infty) - \frac{\sigma B_0^2}{\rho} u' - \frac{\phi}{k'} \left( \nu + \frac{\alpha_1}{\rho} \frac{\partial}{\partial t'} \right) u' + g\beta'_C (C' - C'_\infty) \quad (6.2.1)$$

$$\frac{\partial T'}{\partial t'} = \frac{k_4}{\rho c_p} \frac{\partial^2 T'}{\partial y'^2} - \frac{1}{\rho c_p} \frac{\partial q_r'}{\partial y'} + \frac{Q_0}{\rho c_p} (T' - T'_\infty) \quad (6.2.2)$$

$$\frac{\partial C'}{\partial t'} = D_M \frac{\partial^2 C'}{\partial y'^2} + D_T \frac{\partial^2 T'}{\partial y'^2} - k'_2 (C' - C'_\infty) \quad (6.2.3)$$

with following initial and boundary conditions:

$$u' = 0, \quad T' = T'_\infty, \quad C' = C'_\infty; \text{ as } y' \geq 0 \text{ and } t' \leq 0 \quad (6.2.4)$$

$$u' = U_0 t'^2 \text{ as } t' > 0 \text{ and } y' = 0, \quad T' = \begin{cases} T'_\infty + (T'_w - T'_\infty) t'/t_0 & \text{if } 0 < t' < t_0 \\ T'_w & \text{if } t' \geq t_0 \end{cases},$$

$$C' = \begin{cases} C'_\infty + (C'_w - C'_\infty) t'/t_0 & \text{if } 0 < t' < t_0 \\ C'_w & \text{if } t' \geq t_0 \end{cases}; \quad y' = 0 \quad (6.2.5)$$

$$u' \rightarrow 0, T' \rightarrow T'_\infty, \quad C' \rightarrow C'_\infty; \text{ as } y' \rightarrow \infty \text{ and } t' \geq 0 \quad (6.2.6)$$

Introducing the following dimensionless quantities:

$$y = \frac{U_0 t_0^2 y'}{\nu}, \quad u = \frac{u'}{t_0^2 U_0}, \quad t = \frac{t'}{t_0}, \quad \theta = \frac{(T' - T'_\infty)}{(T'_w - T'_\infty)}, \quad C = \frac{(C' - C'_\infty)}{(C'_w - C'_\infty)}$$

Using dimensionless quantities, equations (6.2.1) to (6.2.6) becomes

$$\frac{\partial^2 u}{\partial y^2} + \alpha \frac{\partial^3 u}{\partial y^2 \partial t} - c \frac{\partial u}{\partial t} - bu + Gr \theta + Gm C = 0 \quad (6.2.7)$$

$$\frac{\partial \theta}{\partial t} = \frac{1+Nr}{Pr} \frac{\partial^2 \theta}{\partial y^2} + \frac{H}{Pr} \theta \quad (6.2.8)$$

$$\frac{\partial C}{\partial t} = \frac{1}{Sc} \frac{\partial^2 C}{\partial y^2} + Sr \frac{\partial^2 \theta}{\partial y^2} - krC \quad (6.2.9)$$

with initial and boundary conditions

$$u = \theta = C = 0, \quad y \geq 0, t \leq 0 \quad (6.2.10)$$

$$u = t^2, \theta = \begin{cases} t, & 0 < t \leq 1 \\ 1, & t > 1 \end{cases}, C = \begin{cases} t, & 0 < t \leq 1 \\ 1, & t > 1 \end{cases} \quad \text{at } y = 0, t > 0 \quad (6.2.11)$$

$$u \rightarrow 0, \theta \rightarrow 0, C \rightarrow 0 \quad \text{at } y \rightarrow \infty, t > 0 \quad (6.2.12)$$

where,

$$\alpha = \frac{\alpha_1}{\rho v t_0}, Gr = \frac{g\beta'_T(T'_w - T'_\infty)}{U_0 t_0}, M^2 = \frac{\sigma B_0^2}{\rho U_0 t_0}, \frac{1}{k_1} = \frac{U_0 v t_0^2 \phi}{k'_1}, Gm = \frac{g\beta'_C(C'_w - C'_\infty)}{U_0 t_0}, Pr = \frac{\rho v c_p}{k},$$

$$Nr = \frac{16\sigma^* T_\infty'^3}{3k k^*}, H = \frac{Q_0 v t_0}{k}, Sc = \frac{v}{D_M}, Sr = \frac{D_T(T'_w - T'_\infty)}{v(C'_w - C'_\infty)}, Kr = t_0 k'_2, c = 1 + \frac{\alpha}{k_1}, b = M^2 + \frac{1}{k_1}$$

$$q_r' = -\frac{4\sigma^*}{3k^*} \frac{\partial T'^4}{\partial y'}, T'^4 \cong 4T_\infty'^3 T' - 3T_\infty'^4, \frac{\partial q_r'}{\partial y'} = -\frac{16\sigma^* T_\infty'^3}{3k^*} \frac{\partial^2 T'}{\partial y'^2}$$

$$\text{For Simplicity, } t_0 = \left(\frac{v}{U_0^2}\right)^{1/5}$$

## 6.2.4 Solution of the Problem

Analytical expression for velocity, temperature and concentration profiles are derived from equations (6.2.9) to (6.2.11) with initial and boundary condition (6.2.12) using the Laplace transform technique.

### 6.2.4.1 Solution of the Problem for ramped temperature and ramped surface concentration

$$\theta(y, t) = f_6(y, t, L, a_1) - f_6(y, t - 1, L, a_1)H(t - 1) \quad (6.2.13)$$

$$C(y, t) = [f_6(y, t, Sc, ScKr) + f_8(y, t, Sc, ScKr) - f_8(y, t, L, a_1)] - [f_6(y, t - 1, Sc, ScKr) + f_8(y, t - 1, Sc, ScKr) - f_8(y, t - 1, L, a_1)]H(t - 1) \quad (6.2.14)$$

$$u(y, t) = [g_1(y, t) + g_2(f_3(t), f_9(y, t, Sc, ScKr)) + g_2(f_4(t), f_9(y, t, L, a_1))] - [g_1(y, t - 1) + g_2(f_3(t - 1), f_9(y, t - 1, Sc, ScKr)) + g_2(f_4(t - 1), f_9(y, t - 1, L, a_1))]H(t - 1) \quad (6.2.15)$$

**6.2.4.2 Solution of the Problem for isothermal temperature and ramped surface concentration**

In this case, the initial and boundary conditions are the same excluding equation (6.2.12) that becomes  $\theta = 1$  at  $y = 0, t \geq 0$ . So, expression of temperature, concentration and velocity profiles are derived for this case using Laplace transform technique, which can be written as

$$\theta(y, t) = f_5(y, t, L, a_1) \quad (6.2.16)$$

$$C(y, t) = [f_6(y, t, Sc, ScKr) - f_6(y, t - 1, Sc, ScKr)H(t - 1) + f_{12}(y, t, Sc, ScKr) - f_{12}(y, t, L, a_1)] \quad (6.2.17)$$

$$u(y, t) = g_1(y, t) + g_2(f_{10}(t), f_9(y, t, L, a_1)) + g_3(f_{11}(t, a_9, a_{10}, a_{11}), f_9(y, t, Sc, ScKr)) - g_3(f_{11}(t - 1, a_9, a_{10}, a_{11}), f_9(y, t - 1, Sc, ScKr)) + g_3(f_{11}(t, a_{30}, a_{31}, a_{32}), f_9(y, t, Sc, ScKr)) \quad (6.2.18)$$

Where

$$f_1(t) = 2t \quad (6.2.19)$$

$$f_2(y, t) = \frac{c}{\alpha} e^{-t/\alpha} \int_0^\infty \operatorname{erfc} \left( \frac{y}{2\sqrt{z}} \right) e^{-cz/\alpha} I_0 \left( \frac{2}{\alpha} \sqrt{(c - ab)zt} \right) dz + \frac{b}{\alpha} \int_0^\infty \int_0^t \operatorname{erfc} \left( \frac{y}{2\sqrt{z}} \right) e^{-\frac{cz+s}{\alpha}} I_0 \left( \frac{2}{\alpha} \sqrt{(c - ab)zs} \right) ds dz \quad (6.2.20)$$

$$f_3(t) = a_{23} + a_{24} e^{b_9 t} + a_{25} e^{b_{10} t} + a_{13} e^{-a_4 t} \quad (6.2.21)$$

$$f_4(t) = a_{26} + a_{27} e^{b_4 t} + a_{28} e^{b_5 t} - a_{20} e^{-a_4 t} \quad (6.2.22)$$

$$f_5(y, t, a, b) = \frac{1}{2} \left[ e^{-y\sqrt{b}} \operatorname{erfc} \left( \frac{y}{2\sqrt{t}} - \sqrt{bt} \right) + e^{y\sqrt{b}} \operatorname{erfc} \left( \frac{y}{2\sqrt{t}} + \sqrt{bt} \right) \right] \quad (6.2.23)$$

$$f_6(y, t, a, b) = \frac{1}{2} \left[ \left( t - \frac{y}{2\sqrt{b}} \right) e^{-y\sqrt{b}} \operatorname{erfc} \left( \frac{y}{2\sqrt{t}} - \sqrt{bt} \right) + \left( t + \frac{y}{2\sqrt{b}} \right) e^{y\sqrt{b}} \operatorname{erfc} \left( \frac{y}{2\sqrt{t}} + \sqrt{bt} \right) \right] \quad (6.2.24)$$

$$f_7(y, t, a, b) = \frac{e^{-at}}{2} \left[ e^{-y\sqrt{\frac{1}{a}(b-a)}} \operatorname{erfc} \left( \frac{y}{2\sqrt{t}} - \sqrt{(b-a)t} \right) + e^{y\sqrt{\frac{1}{a}(b-a)}} \operatorname{erfc} \left( \frac{y}{2\sqrt{t}} + \sqrt{(b-a)t} \right) \right] \quad (6.2.25)$$

$$f_8(y, t, a, b) = a_8 f_5(y, t, a, b) + a_6 f_6(y, t, a, b) + a_7 f_7(y, t, a, b) \quad (6.2.26)$$

$$f_9(y, t, a, b) = f_2(y, t) - f_5(y, t, a, b) \quad (6.2.27)$$

$$f_{10}(t) = -a_{33} + a_{36} e^{b_4 t} + a_{37} e^{b_5 t} \quad (6.2.28)$$

$$f_{11}(t, p, q, r) = p + q e^{b_9 t} + r e^{b_{10} t} \quad (6.2.29)$$

$$f_{12}(y, t, a, b) = a_6 f_5(y, t, a, b) + a_{38} f_7(y, t, a, b) \quad (6.2.30)$$

$$g_1(y, t) = \int_0^t f_2(y, u) f_1(t - u) du \quad (6.2.31)$$

$$g_2(f_i(t), f_j(y, t, a, b)) = \int_0^t f_j(y, u, a, b) f_i(t - u) du \quad (6.2.32)$$

$$g_3(f_i(t, p, q, r), f_j(y, t, a, b)) = \int_0^t f_j(y, u, a, b) f_i(t - u, p, q, r) du \quad (6.2.33)$$

### 6.2.4.3 Skin friction, Nusselt number and Sherwood number

Expressions of Skin friction  $\tau$ , Nusselt number  $Nu$  and Sherwood number  $Sh$  are calculated from equations (6.2.13) to (6.2.18) using the relation

$$\tau_w(t) = -\tau(y, t) \text{ at } y = 0, \tau(y, t) = \left(1 + \alpha \frac{\partial}{\partial t}\right) \frac{\partial u}{\partial y} \Big|_{y=0}, N_u = -\left(\frac{\partial \theta}{\partial y}\right)_{y=0} \text{ and } s_h = -\left(\frac{\partial c}{\partial y}\right)_{y=0} \quad (6.2.34)$$

For ramped wall temperature and ramped surface concentration

$$\frac{\partial u}{\partial y} \Big|_{y=0} = [I_8(t) + I_9(t, Sc, ScKr) + I_9(t, L, a_1)] - [I_8(t - 1) + I_9(t - 1, Sc, ScKr) + I_9(t - 1, L, a_1)]H(t - 1) \quad (6.2.35)$$

$$Nu = -[I_3(t, L, a_1) - I_3(t - 1, L, a_1)]H(t - 1) \quad (6.2.36)$$

$$Sh = -[I_3(t, Sc, ScKr) + I_5(t, Sc, ScKr) - I_5(t, L, a_1)] + [I_3(t - 1, Sc, ScKr) + I_5(t - 1, Sc, ScKr) - I_5(t - 1, L, a_1)]H(t - 1) \quad (6.2.37)$$

For isothermal temperature and ramped surface concentration

$$\frac{\partial u}{\partial y} \Big|_{y=0} = [I_8(t) + I_9(t, L, a_1) + I_{10}(t, a_9, a_{10}, a_{11}, Sc, ScKr) - I_{10}(t - 1, a_9, a_{10}, a_{11}, Sc, ScKr) + I_{10}(t, a_{30}, a_{31}, a_{32}, Sc, ScKr)] \quad (6.2.38)$$

$$Nu = -[I_2(t, L, a_1)] \quad (6.2.39)$$

$$Sh = -[I_3(t, Sc, ScKr) - I_6(t - 1, Sc, ScKr)H(t - 1) + I_{12}(t, Sc, ScKr) - I_{12}(t, L, a_1)] \quad (6.2.40)$$

where,

$$I_1(t) = \frac{df_2(y,t)}{dy} \Big|_{y=0} = \frac{c}{\alpha\sqrt{\pi}} e^{-t/\alpha} \int_0^\infty \frac{e^{-cz/\alpha}}{\sqrt{z}} I_0\left(\frac{2}{\alpha}\sqrt{(c-ab)zt}\right) dz - \frac{b}{\alpha\sqrt{\pi}} \int_0^\infty \int_0^t \frac{e^{-cz+s/\alpha}}{\sqrt{z}} I_0\left(\frac{2}{\alpha}\sqrt{(c-ab)zs}\right) ds dz \quad (6.2.41)$$

$$I_2(t, a, b) = \frac{df_5(y,t)}{dy} \Big|_{y=0} = -\sqrt{b} \operatorname{erf}\left(\sqrt{\frac{b}{a}} t\right) + \sqrt{\frac{a}{\pi t}} e^{-\frac{b}{a}t} \quad (6.2.42)$$

$$I_3(t, a, b) = \frac{df_6(y,t,a,b)}{dy} \Big|_{y=0} = -\sqrt{\frac{a^2}{4b}} \operatorname{erf}\left(\sqrt{\frac{b}{a}} t\right) - t\sqrt{b} \operatorname{erf}\left(\sqrt{\frac{b}{a}} t\right) + \sqrt{\frac{ta}{\pi}} e^{-\frac{b}{a}t} \quad (6.2.43)$$

$$I_4(t, a, b) = \frac{df_7(y,t,a,b)}{dy} \Big|_{y=0} = -e^{-a_4t} \sqrt{(b - a a_4)} \operatorname{erf}\left(\sqrt{\left(\frac{b}{a} - a_4\right) t}\right) + \sqrt{\frac{a}{\pi t}} e^{-\frac{b}{a}t} \quad (6.2.44)$$

$$I_5(t, a, b) = \frac{df_8(y,t,a,b)}{dy} \Big|_{y=0} = a_8 I_2(t, a, b) + a_6 I_3(t, a, b) + a_7 I_4(t, a, b) \quad (6.2.45)$$

$$I_6(t, a, b) = \frac{df_9(y,t,a,b)}{dy} \Big|_{y=0} = I_1(t) - I_2(t, a, b) \quad (6.2.46)$$

$$I_7(t, a, b) = \frac{df_{10}(y,t,a,b)}{dy} \Big|_{y=0} = a_6 I_2(t, a, b) + a_{38} I_4(t, a, b) \quad (6.2.47)$$

$$I_8(t) = \frac{dg_1(y,t)}{dy} \Big|_{y=0} = \int_0^t I_1(u) f_1(t - u) du \quad (6.2.48)$$

$$I_9(t, a, b) = \frac{dg_2\left(\left(f_i(t), f_j(y,t,a,b)\right)\right)}{dy} = \int_0^t I_j(u, a, b) f_i(t - u) du \quad (6.2.49)$$

$$I_{10}(t, p, q, r, a, b) = \frac{dg_2\left(f_i(t,p,q,r), f_j(y,t,a,b)\right)}{dy} = \int_0^t I_j(y, u, a, b) f_i(t - u, p, q, r) du \quad (6.2.50)$$

### 6.2.5 Result and Discussion

The fluid velocity, temperature and concentration are presented for several values of Second grade parameter  $\alpha$ , magnetic field  $M$ , thermo-diffusion  $Sr$ , thermal radiation parameter  $Nr$ , chemical reaction parameter  $Kr$  and Heat generation/absorption  $H$  in Figure 6.2.2 to Figure 6.2.11.

Figure 6.2.2 shows that magnetic field has retarding effect on velocity profile for both thermal conditions. The presence of magnetic parameter generates electric field in the flow field. This is due to point that the application of a magnetic field to fluid gives increase to a resistive-type force (Lorentz force) on the fluid in the boundary layer, which slow down the motion of the fluid. Figure 6.2.3 Show effects of Second grade parameter  $\alpha$  on velocity for both thermal plates. It is seen that velocity decrease throughout the flow field with increase in Second grade parameter  $\alpha$ . It is also noticed that, the thickness of the boundary layer increases if the Second grade parameter decreases. Figure 6.2.4 and Figure 6.2.5 exhibits the effects of thermo-diffusion  $Sr$  on velocity and concentration profile. For both thermal cases, velocity and concentration profiles increases with increase in  $Sr$ . Physically, increase in values of  $Sr$  produces a raise in the mass buoyancy force which results an increase in the value of velocity profile as well as concentration profile, and thus thermo-diffusion tends to accelerate fluid flow throughout the boundary layer region.

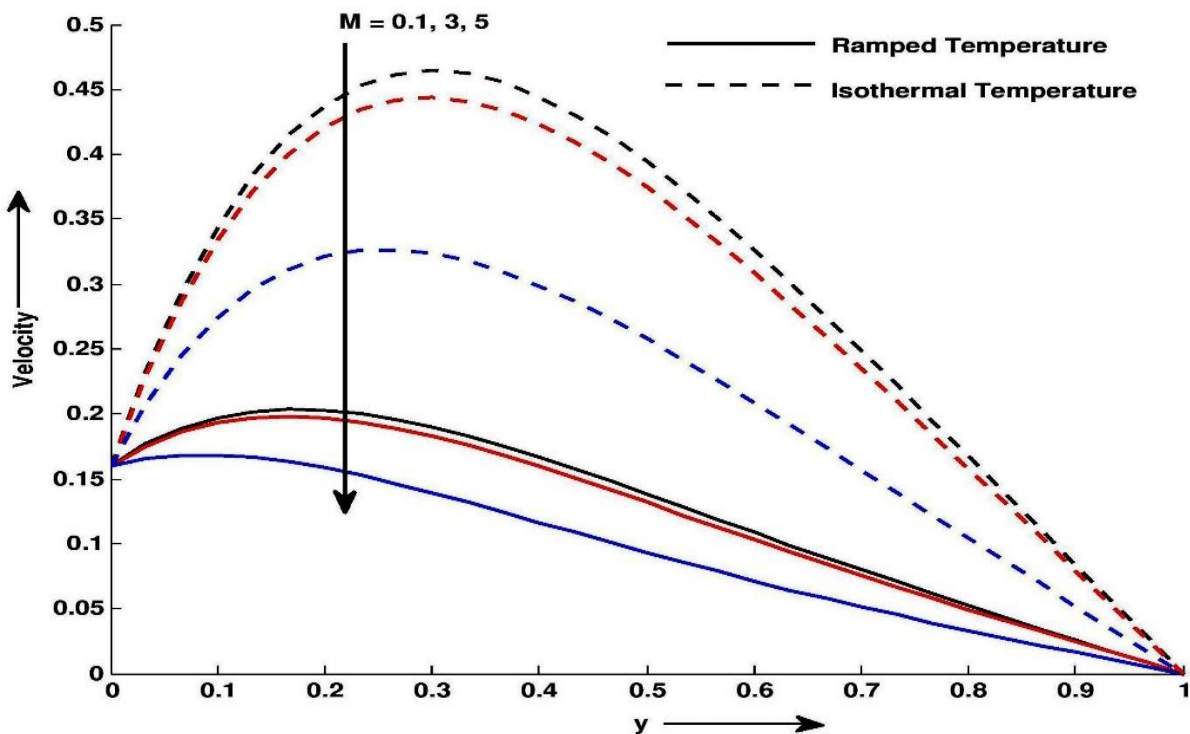


**Figure 6.2.2:** Velocity profile  $u$  for different values of  $y$  and  $M$  at  $k = 0.8, Pr = 7, \alpha = 0.5,$   
 $Sc = 0.66, Gm = 5, Gr = 10, Sr = 3, Kr = 2, H = 3, t = 0.4$  and  $Nr = 5$

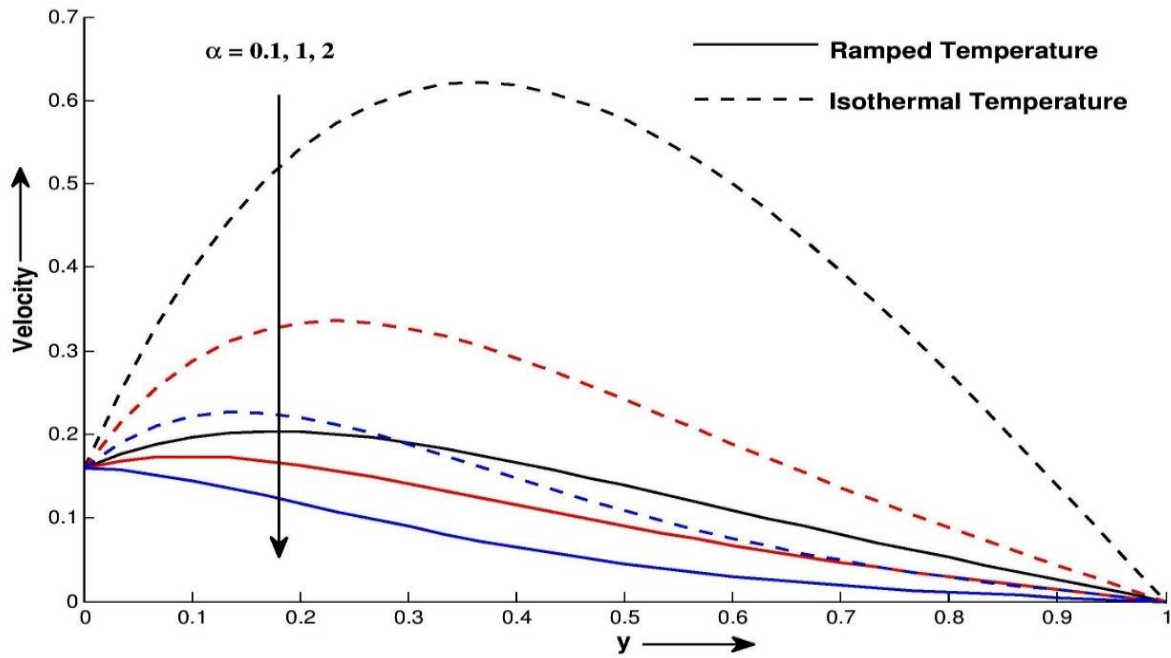


**Figure 6.2.3:** Velocity profile  $u$  for different values of  $y$  and  $\alpha$  at  $k = 0.8, Pr = 7, M = 0.5,$   
 $Sc = 0.66, Gm = 5, Gr = 10, Sr = 3, Kr = 2, H = 3, t = 0.4$  and  $Nr = 5$

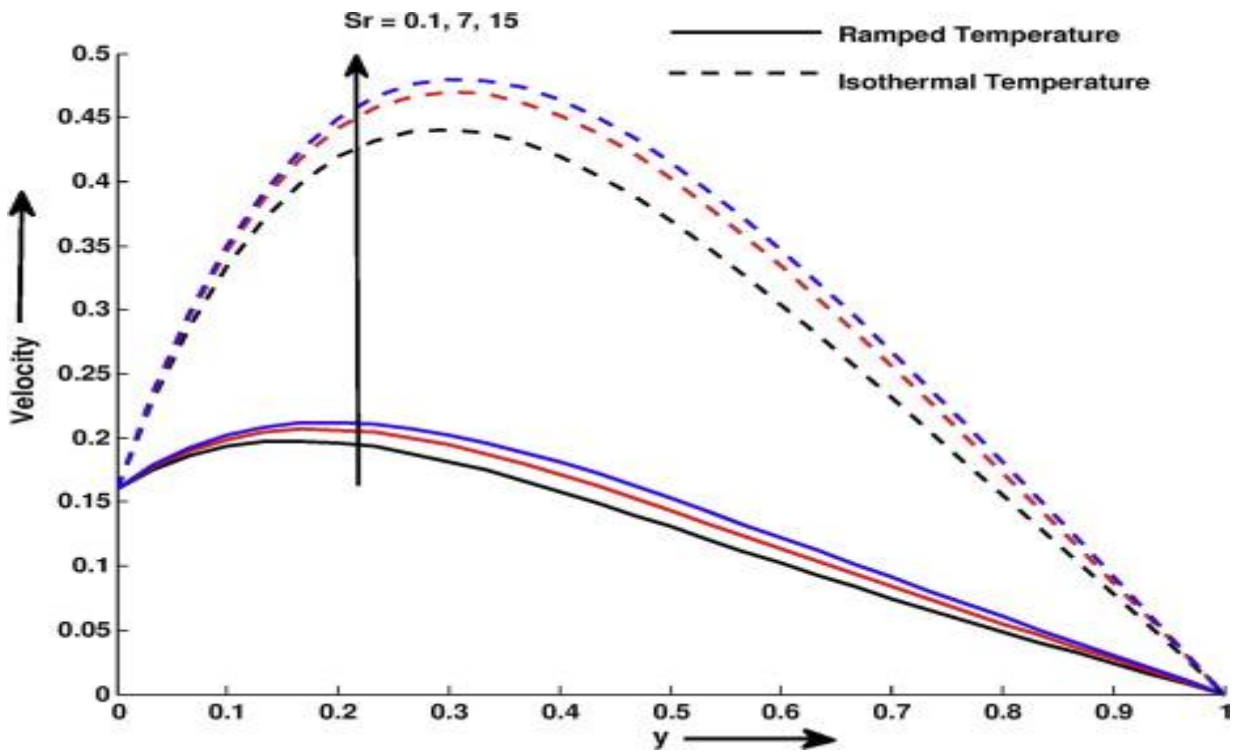


**Figure 6.2.4:** Velocity profile  $u$  for different values of  $y$  and  $Sr$  at  $k = 0.8, Pr = 7, \alpha = 0.5,$   
 $Sc = 0.66, Gm = 5, Gr = 10, M = 0.5, Kr = 2, H = 3, t = 0.4$  and  $Nr = 5$

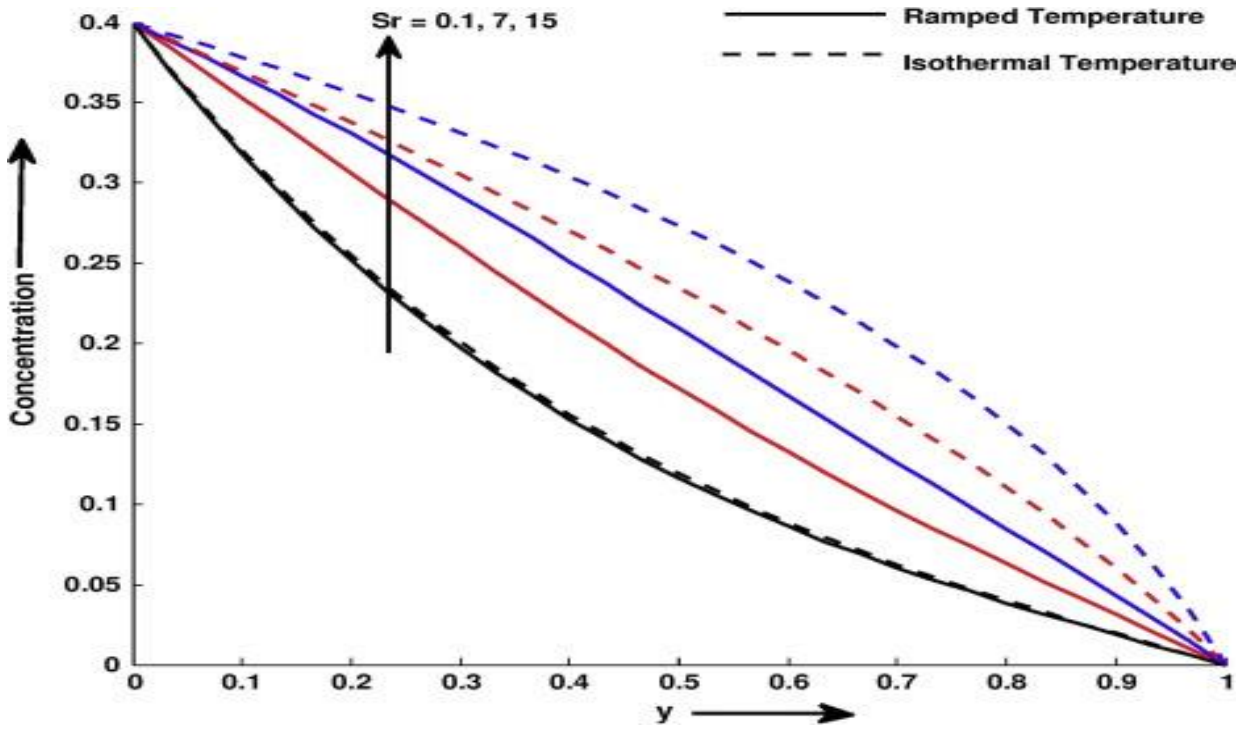


**Figure 6.2.5:** Concentration profile  $C$  for different values of  $y$  and  $Sr$  at  $Pr = 7, Sc = 0.66, Kr = 2, H = 3, t = 0.4$  and  $Nr = 5$

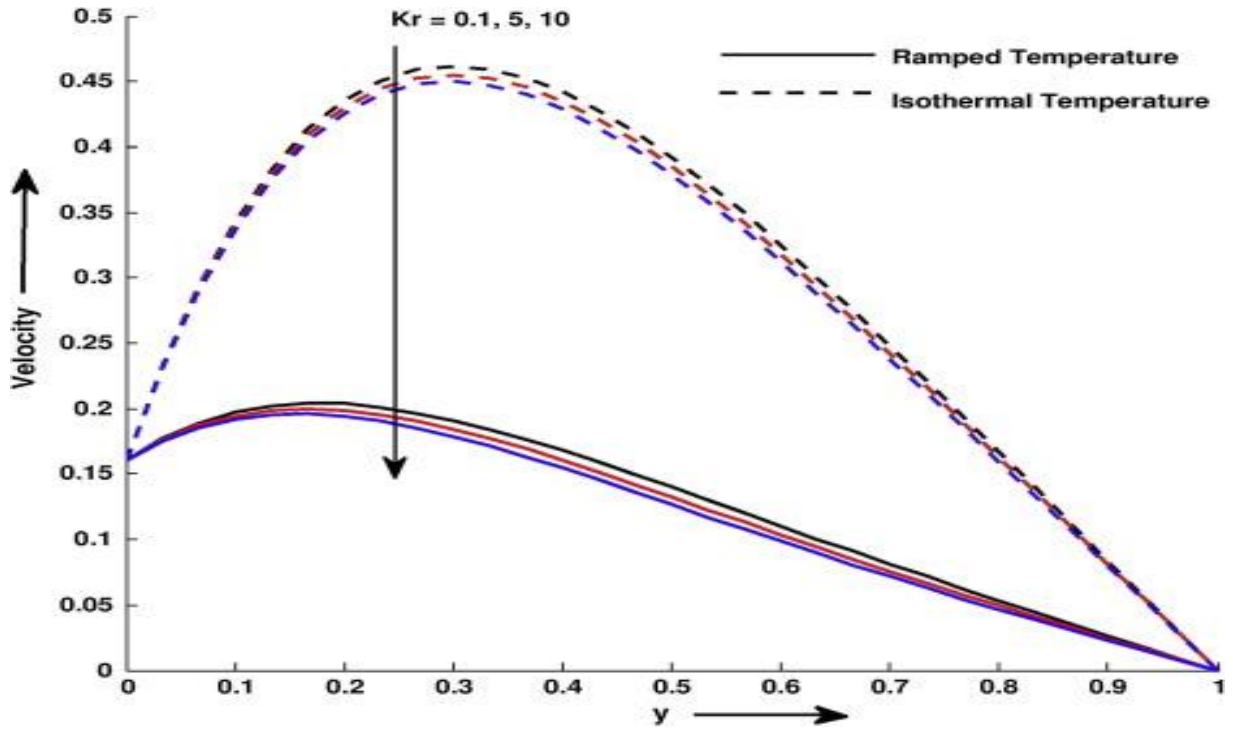


**Figure 6.2.6:** Velocity profile  $u$  for different values of  $y$  and  $Kr$  at  $k = 0.8, Pr = 7, \alpha = 0.5, Sc = 0.66, Gm = 5, Gr = 10, Sr = 3, M = 0.5, H = 3, t = 0.4$  and  $Nr = 5$

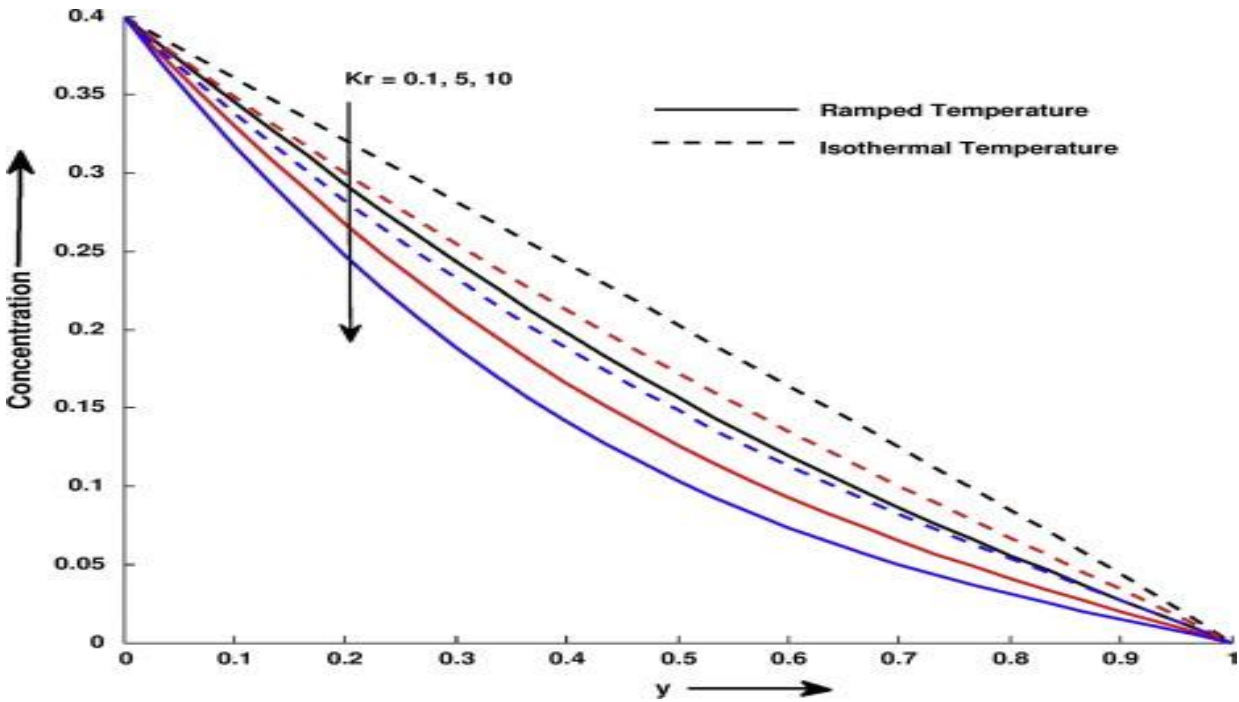


**Figure 6.2.7:** Concentration profile  $C$  for different values of  $y$  and  $Kr$  at  $Pr = 7, Sc = 0.66, Sr = 3, H = 3, t = 0.4$  and  $Nr = 5$ .

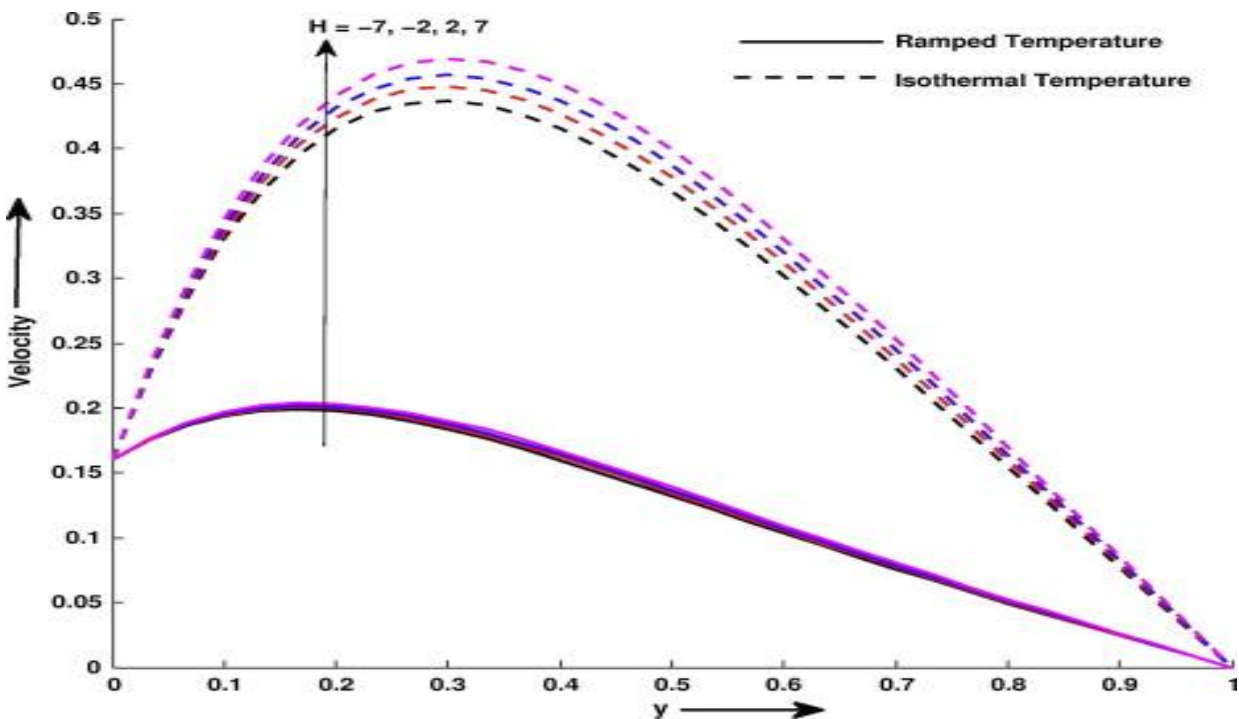


**Figure 6.2.8:** Velocity profile  $u$  for different values of  $y$  and  $H$  at  $k = 0.8, Pr = 7, \alpha = 0.5, Sc = 0.66, Gm = 5, Gr = 10, Sr = 3, Kr = 2, M = 0.5, t = 0.4$  and  $Nr = 5$

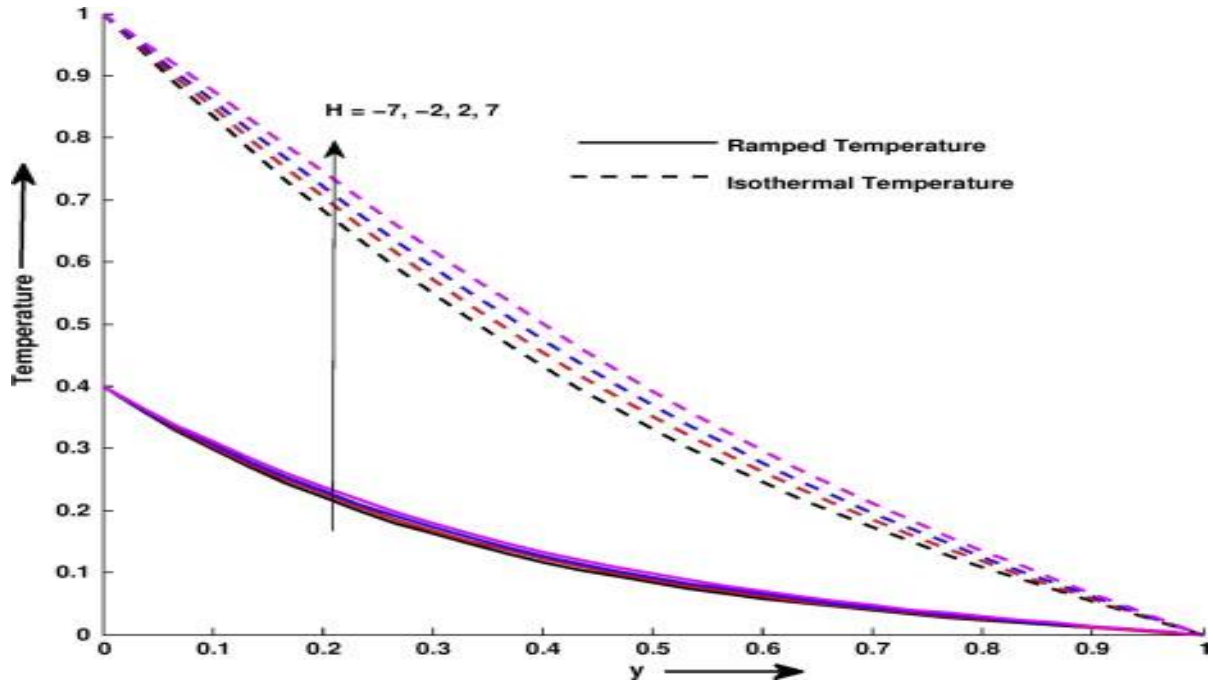


**Figure 6.2.9:** Temperature profile  $\theta$  for different values of  $y$  and  $H$  at  $Pr = 7, t = 0.4$  and  $Nr = 5$

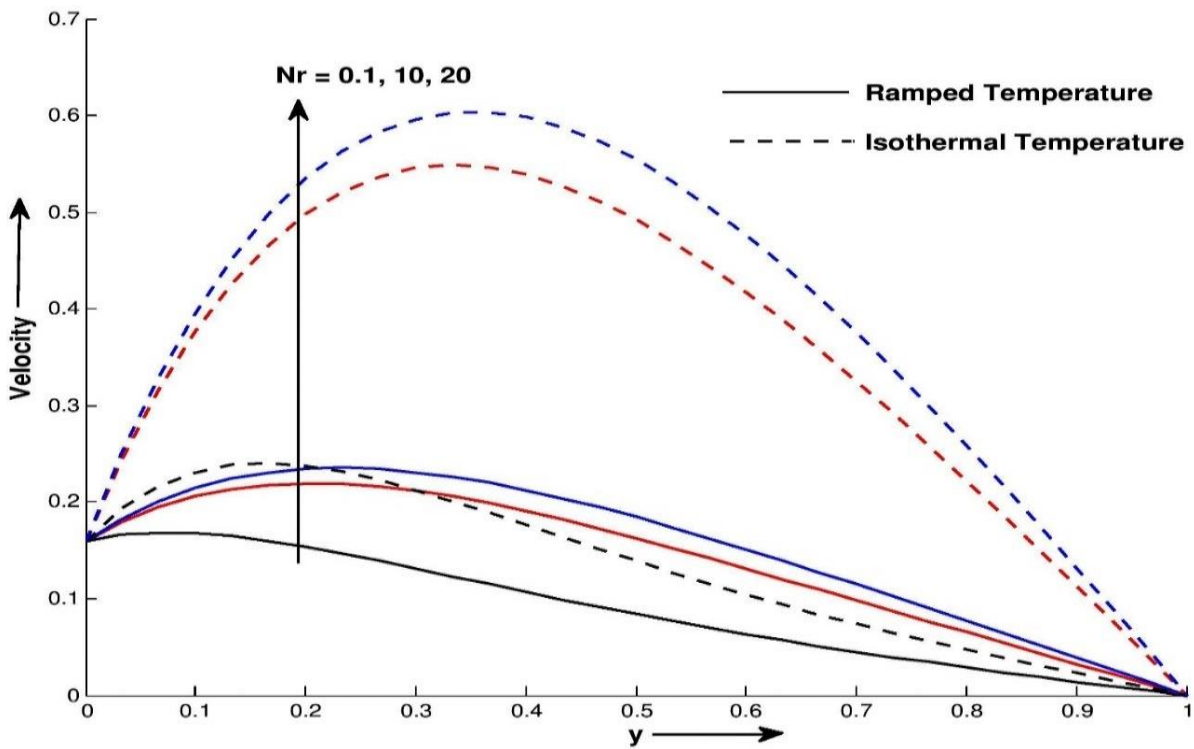


**Figure 6.2.10:** Velocity profile  $u$  for different values of  $y$  and  $Nr$  at  $k = 0.8, Pr = 7, \alpha = 0.5, Sc = 0.66, Gm = 5, Gr = 10, Sr = 3, Kr = 2, H = 3, t = 0.4$  and  $M = 0.5$

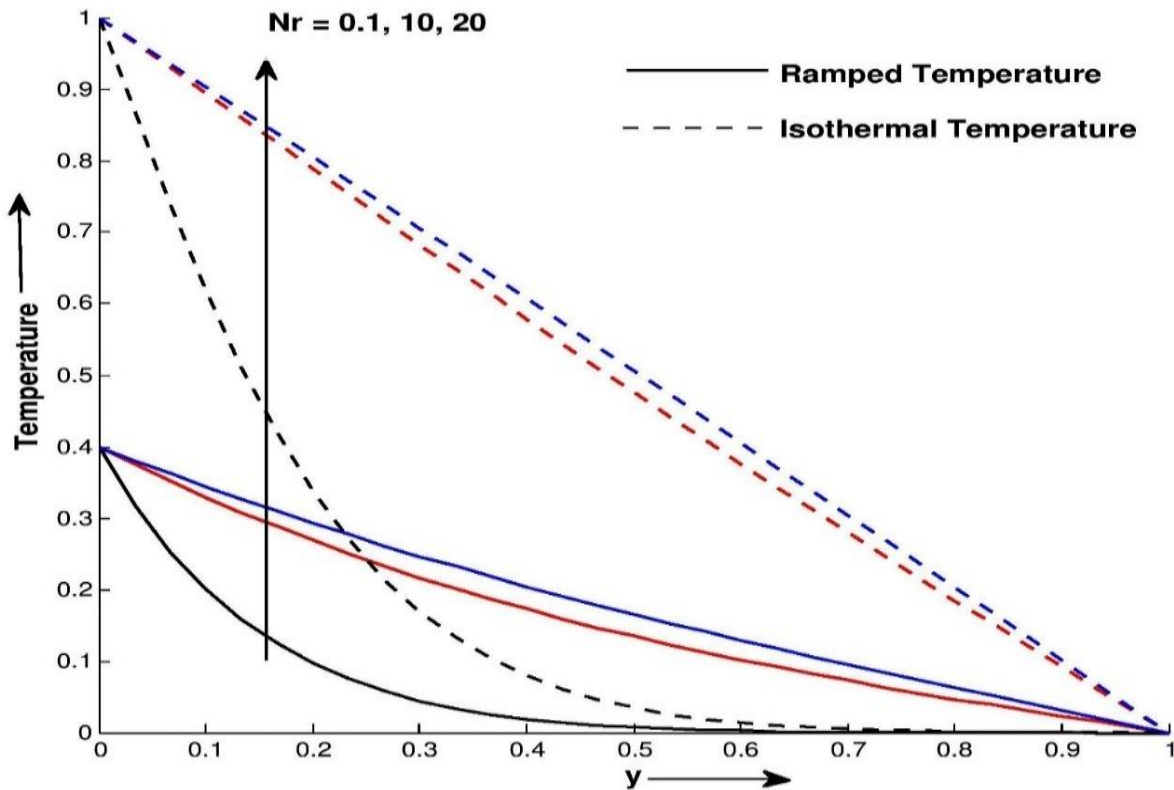


**Figure 6.2.11:** Temperature profile  $\theta$  for different values of  $y$  and  $Nr$  at  $Pr = 7, t = 0.4$  and  $H = 3$

Chemical reaction has retarding influence on fluid flow velocity and concentration profile for both thermal cases as shown in Figure 6.2.6 and Figure 6.2.7. This shows that the destructive reaction  $Kr > 0$  leads to fall in the concentration field which in turn weakens the buoyancy effects due to concentration gradients. Consequently, the flow field is retarded. This occurrence has a superior agreement with the physical realities. These results are in agreement with the results of Kataria and Patel [127]. Figure 6.2.8 and Figure 6.2.9 shows heat generation/absorption  $H$  effects on velocity and temperature profiles. The positive sign shows the heat generation (heat source) whereas negative means heat absorption (heat sink). These results are clearly supported from the physical point of view because heat source implies generation of heat from the surface of the region, hall of the porous is also increase which rises the temperature in the flow field. Therefore, velocity and temperature profiles increase with increase in  $H$  for both thermal plates. Thermal radiation parameter tends to improved velocity and temperature profile as shown in Figure 6.2.10 and Figure 6.2.11. It is observed that radiation parameter decreases thermal buoyancy force, minimizing the thickness of the thermal boundary layer. Therefore velocity and temperature profiles increase with radiation

parameter  $Nr$ . Physically, when the amount of heat generated through thermal radiation parameter increases, the bond holding the components of the fluid particles is easily broken and the fluid velocity will increase. Thus, it is pointed out that the radiation should be minimized to have the cooling process at a faster rate.

**Table 6.2.1:** Nusselt number Variation

$H$	$Nr$	$Pr$	$t$	$Nu$ for Ramped temperature	$Nu$ for isothermal temperature
-1	5	7	0.4	0.7854	1.0181
-2	5	7	0.4	0.7999	1.0716
-3	5	7	0.4	0.8141	1.1242
-1	6	7	0.4	0.7272	0.9426
-1	7	7	0.4	0.6802	0.8817
-1	5	10	0.4	0.9336	1.1974
-1	5	15	0.4	1.1384	1.4479
-1	5	7	0.5	0.8822	0.9226
-1	5	7	0.6	0.9708	0.8532

**Table 6.2.2:** Sherwood number variation

$Sr$	$Sc$	$Pr$	$Kr$	$H$	$Nr$	$t$	$Sh$ for Ramped temperature	$Sh$ for isothermal temperature
2	0.66	7	2	-1	5	0.4	0.1852	0.1399
3	0.66	7	2	-1	5	0.4	-0.0838	-0.1518
4	0.66	7	2	-1	5	0.4	-0.3528	-0.4435
2	0.8	7	2	-1	5	0.4	0.1744	0.1291
2	1.0	7	2	-1	5	0.4	0.1569	0.1131
2	0.66	10	2	-1	5	0.4	0.0308	-0.0273
2	0.66	15	2	-1	5	0.4	-0.1935	-0.2775
2	0.66	7	3	-1	5	0.4	0.2737	0.2755
2	0.66	7	4	-1	5	0.4	0.3555	0.3937
2	0.66	7	2	-2	5	0.4	0.1702	0.0854
2	0.66	7	2	-3	5	0.4	0.1553	0.0317
2	0.66	7	2	-1	6	0.4	0.2437	0.2076

2	0.66	7	2	-1	7	0.4	0.2897	0.2605
2	0.66	7	2	-1	5	0.5	0.2534	0.3450
2	0.66	7	2	-1	5	0.6	0.3261	0.5250

**Table 6.2.3:** Comparison of Nusselt number with Ref. [148] at  $Pr = 0.71$ 

$Nr$	$\phi = -H/Pr$	$t$	$Nu$ for ramped temp. Ref [148]	$Nu$ for ramped temp.	$Nu$ for isothermal temp. Ref [148]	$Nu$ for isothermal temp.
2	3	0.3	0.38368	0.3837	0.89492	0.8949
2	3	0.5	0.55828	0.5583	0.85907	0.8591
2	3	0.7	0.72887	0.7289	0.84872	0.8487
2	1	0.5	0.44983	0.4498	0.56755	0.5675
2	3	0.5	0.55828	0.5583	0.85907	0.8591
2	5	0.5	0.65207	0.6521	1.09210	1.0921
2	3	0.5	0.55828	0.5583	0.85907	0.8591
4	3	0.5	0.43244	0.4324	0.66543	0.6654
6	3	0.5	0.36548	0.3655	0.56239	0.5624

**Table 6.2.4:** Comparison of Sherwood number with Ref. [149] at  $Sr = 0$ 

$t$	$Kr$	$Sc$	Sh for ramped temp. Ref [149]	Sh for ramped temp.	Sh for isothermal temp. Ref [149]	Sh for isothermal temp.
0.3	0.2	0.22	0.295649	0.2956	0.525702	0.5257
0.5	0.2	0.22	0.386593	0.3866	0.428415	0.4284
0.7	0.2	0.22	0.463189	0.4632	0.379505	0.3796
0.3	2.0	0.22	0.344659	0.3447	0.839945	0.8399
0.5	2.0	0.22	0.488076	0.4881	0.785973	0.7860
0.7	2.0	0.22	0.625355	0.6254	0.757863	0.7579
0.3	5.0	0.22	0.416933	0.4169	1.1897	1.1897
0.5	5.0	0.22	0.628694	0.6287	1.12945	1.1294
0.7	5.0	0.22	0.838894	0.8389	1.09522	1.0952

The variation of the Nusselt number and Sherwood number are shown in Table 6.2.1 and Table 6.2.2 for various values of the governing parameters. It is observed from Table 6.4.1 that, for both thermal cases, thermal radiation parameter tends to reduce the Nusselt number, whereas heat absorption parameter  $H$  and Prandtl number  $Pr$  have reverse outcome on it. It is also seen that, for ramped wall temperature, time variable  $t$  tends to improve rate of heat transfer, whereas for isothermal plates, time variable  $t$  have reverse effect on it. Table 6.2.2 illustrates the effects of  $Pr, Sc, Sr, R, Kr, H$  and  $t$  on Sherwood number  $Sh$ . For both thermal conditions, Sherwood number increase with increase in thermal radiation parameter  $Nr$ , chemical reaction  $Kr$  and time variable  $t$  whereas decrease with increase in Soret number  $Sr$ , Schmidt number  $Sc$ , Prandtl number  $Pr$  and heat generation/absorption  $H$ . Table 6.2.3 validates our outcomes in terms of Nusselt number as it displays strong agreement with Seth et al. [148] whereas Table 6.2.4 strengthens values of Sherwood number by matching with those of Seth et al. [149].

### 6.2.6 Conclusion

The most important concluding remarks can be summarized as follows:

- Magnetic field  $M$ , Second grade parameter  $\alpha$  and chemical reaction parameter  $Kr$  delays velocity of the fluid flow throughout the boundary layer.
- Thermo-diffusion  $Sr$ , thermal radiation parameter  $Nr$  and heat generation parameter  $H$  tends to improve velocity profile throughout the flow field.
- Temperature profile increase tendency with heat generation parameter  $H$  and thermal radiation parameter  $Nr$ .
- Chemical reaction  $Kr$  tends to reduce mass transfer process, whereas thermo-diffusion  $Sr$  has reverse effect on it.
- Thermal radiation parameter tends to reduce rate of heat transfer, whereas heat generation parameter  $H$  and Prandtl number  $Pr$  has reverse effect on it.
- Thermo-diffusion  $Sr$  tends to decrease rate of mass transfer, whereas chemical reaction and time variable  $t$  have reverse effects on it.